Tesis Doctoral

Ingeniería Química

Modeling and Control of Solar Fields with Partial Radiation

Autor: Sergio Jesús Navas Herrera

Directores: Francisco Rodríguez Rubio
Pedro Ollero de Castro

Dpto. Ingeniería de Sistemas y Automática
Escuela Técnica Superior de Ingeniería
Universidad de Sevilla

Sevilla, 2018

UNIVERSIDAD DE SEVILLA

ESCUELA TÉCNICA SUPERIOR DE INGENIERÍA

PHD THESIS:

MODELING AND CONTROL OF SOLAR FIELDS WITH PARTIAL RADIATION

Thesis for the Degree of Doctor of Philosophy

Sergio Jesús Navas Herrera

Supervised by:
Prof. Francisco Rodríguez Rubio
Prof. Pedro Antonio Ollero de Castro

Departamento de Ingeniería de Sistemas y Automática
Programa de Doctorado en Ingeniería Automática, Electrónica y de Telecomunicación

Seville, Spain 2018

Tesis Doctoral: Modeling and Control of Solar Fields with Partial Radiation

Autor: Sergio Jesús Navas Herrera

Directores: Francisco Rodríguez Rubio y Pedro Antonio Ollero de Castro

El tribunal nombrado para juzgar la Tesis arriba indicada, compuesto por los siguientes doctores:

Presidente:

Vocales:

Secretario:

acuerdan otorgarle la calificación de:

El Secretario del Tribunal

Fecha:

Dedicado a
mis amigos y a mi familia

Agradecimientos

En primer lugar, quisiera mostrar mi agradecimiento a mis directores de Tesis, Francisco Rodríguez Rubio y Pedro Ollero. Gracias a sus consejos y recomendaciones ha sido posible sacar adelante esta Tesis, aun cuando en ciertas ocasiones no consiguieramos ponernos de acuerdo. A Francisco le quiero agradecer especialmente su gran trabajo de dirección, ya que en ningún momento he tenido dudas sobre el objetivo final de la Tesis y los pasos a seguir para alcanzarlo. Con respecto a Pedro, tengo muchas cosas que agradecerle, ya que para mi más que un profesor, ha sido un maestro. Él es quién me hizo descubrir mi gusto por el control de procesos, y quién me enseñó a pensar como un ingeniero gracias a esos largos debates sobre control y simulación. Por último y no menos importante, gracias a él he podido dedicarme durante mi tesis, aunque fuera brevemente, a la docencia de control y simulación de procesos, que sin lugar a dudas es mi vocación.

También he de agradecer al profesor João Miranda Lemos su gran dedicación durante mi breve estancia en Lisboa. Gracias a él aprendí mucho sobre control predictivo, lo cual me permitió seguir adelante con la Tesis hasta su posterior culminación. Además he de agradecer sus minuciosas revisiones a nuestros artículos y sus buenos consejos para favorecer su publicación.

Durante el período en el que he desarrollado mi Tesis he tenido la suerte de conocer o tener a mi lado a personas increíbles que han hecho posible el que esta Tesis haya salido adelante. En especial destacan Gracia, Miguel y Javi, ellos han sido como una familia para mi durante todo este tiempo, siempre dispuestos a ayudarnos los unos a los otros. También quiero agradecer a mis compañeros de la becaría (María, Jesús y Fran) aquellas memorables charlas que nos despejaban para poder seguir adelante. Finalmente aunque fue el último en llegar, quiero agradecer a Fran Baena el que siempre supiera qué decir para alegrarme el día. Por último, no puedo olvidarme del profesor Fernando Castaño, quién a pesar de su reticencia me ha enseñado muchas cosas.

También quisiera dar las gracias, a la Universidad de Sevilla, al Ministerio de Economía y Competitividad del gobierno de España por la ayuda recibida por medio del proyecto “Estimación y Predicción Distribuida de la Radiación para Control de Campos Solares (CODISOL)” (DPI2013-44135-R) y a la Asociación de Investigación y Cooperación Industrial de Andalucía (AICIA) por la financiación durante el tiempo de realización de la tesis.

Finalmente le doy las gracias a todos mis amigos ajenos a la escuela, ya que gracias a vosotros he tenido una vía de escape cuando la frustración y el estrés aumentaban en demasía. ¡Gracias a todos!

Resumen

El objetivo principal de esta tesis es el modelado, simulación y control óptimo de campos solares de colectores cilindro-parabólicos durante situaciones de radiación parcial, es decir, cuando diferentes zonas del campo reciben distintos niveles de radiación solar. Hoy en día, las plantas comerciales tienen dificultades a la hora de operar el campo de colectores cuando a lo largo del día se produce el paso de nubes esporádicas que afectan a diferentes zonas del mismo. En esta tesis se estudian las posibles soluciones al problema de control de este tipo de campos solares, mediante técnicas de control avanzado. En primer lugar se ha realizado un modelo completo del campo solar teniendo en cuenta todos los lazos del campo de forma individual. Además también se ha realizado un modelo para simular el paso de las nubes a través del campo y un modelo del ciclo de potencia utilizado por el campo para producir la potencia eléctrica.

Estos modelos se han utilizado en un primer estudio orientado a optimizar la producción de potencia eléctrica. Para ello se ha calculado para cada valor de radiación solar cual es el valor de la temperatura de salida del campo solar que maximiza la potencia eléctrica producida (Paper 1). Las conclusiones obtenidas en este primer estudio, sirvieron para desarrollar un control óptimo del campo que maximizara la potencia eléctrica generada por el mismo. La estrategia de control propuesta se basó en la utilización de un "Model Predictive Control" (MPC), el cual hace uso de un modelo de predicción del paso de las nubes y del campo de colectores para calcular el caudal de aceite óptimo (que para un determinado valor de radiación solar se corresponde con el valor óptimo de temperatura al ser variables dependientes), de forma que maximice la potencia generada. Este MPC se ha probado con dos configuraciones diferentes; una en la que el controlador manipula el caudal total de aceite, el cual luego se divide entre todos los lazos por igual, y otra en la que manipula el caudal que pasa por cada uno de los lazos de forma individual. Los resultados de simulación obtenidos con ambas configuraciones del MPC se compararon con los de la estrategia de control utilizada habitualmente por los campos solares comerciales, basada en mantener una temperatura de

operación del aceite de salida del campo en torno a 400°C, que es el máximo permitido para evitar la degradación del aceite (Paper 2). Con este estudio se puso de manifiesto un problema de operación en el campo cuando se utiliza la estrategia de mantener constante la temperatura del aceite de salida del campo estando parte del mismo cubierto por nubes, el cual consiste en la aparición de picos de temperatura, especialmente en aquellos lazos no afectados por las nubes. El estudio y resolución de este problema dio como resultado a la publicación de un artículo en un congreso (Congress Paper).

Finalmente, para terminar con los objetivos propuestos en esta tesis, se decidió aplicar el proceso de optimización desarrollado anteriormente a una planta solar con sistema de almacenamiento de sales fundidas. Para ello se incorporó al modelo actual del campo un modelo para el sistema de almacenamiento, compuesto por dos tanques de sales fundidas y un intercambiador de calor. También se modificó el modelo del ciclo de potencia para adaptarlo a una producción menor de potencia eléctrica ya que parte de la misma iba a estar destinada a ser almacenada. Con esta nueva configuración de la planta solar el objetivo de la optimización consiste en maximizar la cantidad de energía térmica almacenada mientras se mantiene constante la producción de potencia eléctrica, ésto se debe a que en este caso el objetivo de optimización es mantener la producción eléctrica el máximo número de horas posible, lo cual se consigue maximizando la energía térmica almacenada (teniendo en cuenta un valor de temperatura mínima que luego permita transformarla eficientemente en energía eléctrica). De nuevo se utilizó un MPC para resolver este problema de optimización y los resultados obtenidos se compararon igualmente con la estrategia de control utilizada por las plantas comerciales de mantener la temperatura del aceite de salida del campo en un valor constante y próximo a los 400°C (Paper 3).

Abstract

The main goal of this thesis is the modeling, simulation, and control of parabolic trough solar collector fields during situations of partial radiation, which means that different parts of the solar field receive different degrees of solar radiation. Nowadays, for commercial plants it is difficult to operate this type of fields when some clouds are passing over it, and therefore creating zones with different levels of solar radiation. For that reason, this thesis aims to propose new control strategies that can allow solar collector fields to operate during days with partial radiation. First, a complete model of the solar collector field was made, varying some parameters of an existing one and modeling all the field loops individually. In addition, a simple model to simulate the passage of the clouds and another one to simulate the power cycle used by the solar plant to produce electrical power were made.

Once these models were finished, they were used to study the steady state optimization of the electrical power production. This study is based on the calculation of the optimum operating temperature that maximizes the electrical power generated for each value of the solar radiation (Paper1). After seeing the conclusions obtained by this first study, they were applied to the development of an optimal controller that could achieve this maximization. The proposed control strategy consisted of a MPC that uses predictions of the future clouds and the model of the solar field to calculate the optimal oil flow (for a determined value of solar radiation it leads to the optimal temperature due to the fact that they are dependent variables) that maximizes the power generated. This MPC was assessed with two different configurations; the first one manipulates the total oil flow, which is then equally distributed among the loops, whereas the second one manipulates individually the oil flow of each loop. The simulation results obtained with both MPC configurations were compared against the ones obtained with the typical control strategy used in the commercial fields, based on keeping constant the outlet oil temperature at a value around 400°C, which is the maximum allowable one in order to prevent the oil degradation (Paper 2). When these simulations were being carried out, an operating problem of the solar field related to the use of the constant outlet oil temperature control strategy when it is covered by clouds was discovered. The problem consists of the appearance of temperature peaks in the loops that are not affected by the cloud and was studied and solved in a congress paper (Congress Paper).

Finally, in order to fulfill the thesis objectives, the optimization process developed before was applied to a solar plant with a thermal storage system based on molten salts. For that reason, a new model for the storage system composed of two molten salt tanks and a heat exchanger was added to the complete plant model. Besides, the power cycle model was modified to lower its design electrical power production as some of the energy was going to be stored. With this new configuration of the solar plant the optimization objective is to maximize the thermal energy stored while keeping constant the electrical power production. Again, a MPC was used to solve the optimization and the results were compared against the control strategy of keeping constant the outlet oil temperature, as in the previous case (Paper 3).

List of Publications

Journal papers

- Sergio J. Navas, Pedro Ollero, and Francisco R. Rubio.
  Optimum Operating Temperature of Parabolic Trough Solar Fields.
  Solar Energy. Volume 158, 295-302, 2017.
  DOI:https://doi.org/10.1016/j.solener.2017.09.022

- Sergio J. Navas, Francisco R. Rubio, Pedro Ollero, and João M. Lemos.
  Optimal Control Applied to Distributed Solar Collector Fields with Partial Radiation.
  Solar Energy. Volume 159, 811-819, 2018.
  DOI:https://doi.org/10.1016/j.solener.2017.11.052

- Francisco R. Rubio, Sergio J. Navas, Pedro Ollero, João M. Lemos, and Manuel G. Ortega.
  Optimal Control Applied to Distributed Solar Collector Fields.
  Revista Iberoamericana de Automática e Informática Industrial (RIAI).
  Volume 15, 327-338, 2018.
  DOI:https://doi.org/10.4995/riai.2018.8944

- Sergio J. Navas, Francisco R. Rubio, Pedro Ollero, and João M. Lemos.
  Control of a Distributed Solar Collector Field with Thermal Energy Storage and Partial Radiation.
  Paper under review submitted to the journal "Journal of Process Control".

Congress papers

- Sergio J. Navas, Francisco R. Rubio, and Pedro Ollero.
  Modelado y Simulación de un Campo Solar con Paso de Nube.
  XXXVI Jornadas de Automática, 2-4 de Septiembre de 2015. Bilbao.
  556-559.

- Sergio J. Navas, Francisco R. Rubio, Pedro Ollero, and Manuel G. Ortega.
  Modeling and Simulation of Parabolic Trough Solar Fields with Partial Radiation.
  European Control Conference (ECC), 2016, 31-36.
  DOI:10.1109/ECC.2016.7810259.

- Sergio J. Navas, Francisco R. Rubio, and Pedro Ollero.
  Optimum Control of Parabolic Trough Solar Fields with Partial Radiation.
  IFAC-PapersOnLine 50 (1), 109-114.
  DOI:https://doi.org/10.1016/j.ifacol.2017.08.019

- Sergio J. Navas, Francisco R. Rubio, Pedro Ollero, and João M. Lemos.
  Optimal Control of Solar Thermal Plants with Energy Storage.
  Accepted in the European Control Conference (ECC), 2018.

Contents

List of Figures

List of Tables

Chapter 1

Introduction

A parabolic trough solar collector field is a system that allows to transform the solar energy into thermal energy. This type of solar fields consists of a several collectors grouped in loops that concentrate the solar energy into a pipe through which a synthetic oil circulates with the purpose to be heated. Once the oil is heated it is sent to the power cycle where its thermal energy is used to generate high pressure steam that then is expanded in a turbine to generate electrical power. Due to the way it works, it is clear that the outlet oil temperature is a key factor for the operation of the field. Therefore, this temperature has to be carefully selected and controlled in order to ensure a good performance. The only variable that can be manipulated to control the temperature is the oil flow circulating through each loop; for a certain value of solar radiation the lower the oil flow, the higher the oil temperature, and vice versa.

Nowadays, commercial concentrated solar plants (CSP) operate at a constant value of outlet oil temperature during all the available operation hours. The value of the temperature selected used to be around the maximum allowable one, which is 400°C, in order to prevent the synthetic oil degradation. This value of temperature matches the one used for the plant design, and corresponds to the maximum value of solar radiation. At the maximum value of the solar radiation, it is the maximum value of the outlet oil temperature the one that allows the maximum production of electrical power. However, during the day the value of the solar radiation varies, due to the variation of the sun position or the passage of clouds over it (figure 1.1), and therefore it is necessary to study if keeping constant this value of temperature for the daily operation of the plant is the optimal way to operate it. Consequently, this thesis comes up with the aim to study the optimal way to operate this type of plants. There are some previous studies that were used as starting point, like [4]-[2] and [3], where a review of the most used control strategies is presented. Other control strategies were also reviewed [1]-[6] and [7]. Nevertheless, all these studies have in common the control objective of keeping the outlet oil temperature at its reference value, whereas in this thesis the control objective is either the maximization of the electrical power or to keep it its demanded values. For that reason, there is no comparison in this thesis between that control strategies and the new ones proposed here. Finally, the closest study to the one made in this thesis is presented in [5], where a first approach to the optimal operation of this type of plants was made.

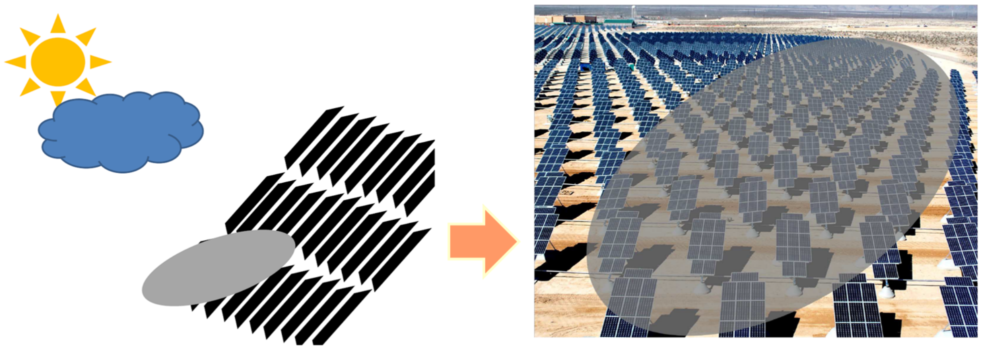

Figure 1.1: Example of a solar field covered by the passage of a cloud

The study of this thesis has been developed in three stages. The first one consisted in a steady state study of the optimal operating temperature (Paper 1) in order to see if to operate the plant at the maximum value of oil outlet temperature for the entire operation produces the maximum amount of electrical power.The results showed that it is better to change the operating temperature according to the value of the incident solar radiation. The second stage was to develop control strategies that can adapt the operating temperature of the plant to the value of the incident solar radiation in real time, a necessity due to the sudden changes in the value of the incident solar radiation that the passage of the clouds can generate. These new control strategies were assessed against the control strategy used in commercial plants that keep constant the operating temperature of the plant during the entire operation with the aim of maximizing the electrical power production in plants without thermal storage (Paper 2). The last stage was to apply a control strategy similar to the one assessed in the previous stage of the study to a plant with thermal storage system. In this case the aim of the control strategy was to maximize the thermal energy stored (in order to extend the operation of the plant after the sunset while keeping the electrical power production close to the reference value selected for each day. This last new control strategy was also compared to the one used by commercial plants to see the level of improvement that can be achieved, and therefore to study if it would be worth to use it in commercial plants (Paper 3).

This study was carried out using the model of a pilot scale solar plant composed of a solar collector field, a power cycle, and a thermal storage system. The model of the solar collector field is the same used for the ACUREX field, but modeling independently all of its loops, which have been increased from 10 to 24, and increasing the length of each one from 172 m to 480 m. This model also includes the modeling of the passage of clouds throughout the field, which modifies the incident solar radiation that reaches every part of the field depending on if that part is covered or not by a cloud. The model of the power cycle consist of a super-heater, a boiler, an economizer and a steam turbo-generator. The super-heater, the boiler, and the economizer were modeled with a steady state energy balance, whereas the steam turbo-generator was modeled using the Willan's Line Method [8]. The dynamic of the power cycle model was assumed to be the slowest one of its components (the boiler), calculated using a simulation software, and added to the steady state model. Finally, the model of the thermal storage system consists of two tanks containing molten salts and a heat exchanger where the heat transfer is produced. The storage tanks are modeled using a mass and an energy balance, while the heat exchanger is modeled in the same way that the power cycle ones.

The control strategies assessed in this thesis are based on model predictive control. The selection of this type of control strategies is due mainly to the need of implementing a real time optimization to reject the disturbances created by the passage of clouds, and to maximize the use of the energy collected by the field. This control objective was achieved using nonlinear MPC subject to constraints. Nonetheless, for each different configuration of the solar plant a different formulation for the MPC was used. These different control strategies were always compared to the strategy most used in commercial plants, which consists of a PI controller followed by a series feedforward.

The Thesis is organized as follows:

- **Chapter 2** enumerates the objectives of the Thesis and gives a brief explanation of them.

- **Chapter 3** presents a summary of the global results of the Thesis, starting from the study of the steady state optimum operating temperature of the solar field, following with the application of that study to develop an optimal control strategy which maximizes the electrical power produced, and ending with the assessment of an optimal control strategy applied to a solar plant with thermal storage.

- **Chapter 4** is a brief summary of the conclusions achieved during the development of the studies that this Thesis is composed of. These conclusions are divided according to the stage of the study where they were obtained.

- **Chapter 5** is the paper where the study of the steady state optimum operating temperature is described in detail. In addition, the complete models of the solar collector field, the passage of clouds, and the power cycle are presented.

- **Chapter 6** is the paper where an optimal control strategy to maximize the electrical power production is developed and assessed. This strategy consists of a nonlinear MPC that uses a simpler model of the solar field and the power field, subject to constraints. Two forms of MPC were tested, one that manipulates the total oil flow circulating through the field, and another one that manipulates the oil flow circulating through each loop.

- **Chapter 7** is the paper where the optimal control strategy studied in the previous paper is applied to a solar plant with thermal storage. However, in this case the control objective is to maximize the thermal energy stored while keeping the electrical power production at its demanded value. The model of the thermal storage system is also presented in this paper.

- **Chapter 8** is a paper presented at a congress that handles the problem of the appearance of temperature peaks. The problem is analyzed and solved by the use of a nonlinear MPC controller subject to temperature constraints.

Bibliography

[1] Barão, M., Lemos, J. and Silva, R. (2002). *Reduced complexity adaptive nonlinear control of a distributed collector solar field.* Journal of Process Control, 12-1, 131-141.

[2] Camacho, E. F., Rubio, F. R., Berenguel, M. and Valenzuela, L. (2007). *A survey on control schemes for distributed solar collector fields. Part I: Modeling and basic control approaches.* Solar Energy, 81-10, 1240-1251.

[3] Camacho, E. F., Rubio, F. R., Berenguel, M. and Valenzuela, L. (2007). *A survey on control schemes for distributed solar collector fields. Part II: Advanced control approaches.* Solar Energy, 81-10, 1252-1272.

[4] Camacho, E. F., Berenguel, M., Rubio, F. R. and Martínez, D. (2012). *Control of solar energy systems, first ed.* Springer-Verlag, London.

[5] Camacho, E. F. and Gallego, A. (2013). *Optimal operation in solar trough plants: A case study.* Solar Energy, 95, 106-117.

[6] Cirre, C., Berenguel, M., Valenzuela, L. and Camacho, E. F. (2007). *Feedback linearization control for a distributed solar collector field.* Control Engineering Practice, 15-12, 1533-1544.

[7] Lima, D., Normey-Rico, J. and Santos, T. (2016). *Temperature control in a solar collector field using filtered dynamic matrix control.* ISA Transactions, 62, 39-49.

[8] Smith, R. (2005). *Chemical process design and integration.* Wiley.

Chapter 2

Objectives

This thesis aims to propose new control strategies that can allow solar collector fields to operate optimally during days with partial radiation, mainly due to the passage of clouds over the field. In order to accomplish this goal, the specific objectives of the thesis are:

- *The modeling and simulation of a solar thermal plant.* This plant consists of a model of a solar collector field that takes into account all the loops individually, instead of modeling only one loop and extrapolating the results for the other loops of the field; as well as a simple model to simulate the passage of the clouds, a power cycle model to determine the electrical power produced by the field, and a model of the thermal storage system (Paper 1 and Paper 3).

- *The study of the optimum steady state operating temperature of the solar collector field.* It is known that at high values of incident solar radiation the best operating temperature, which is the one that maximizes the electrical power production, is the highest allowable one (400°) due to the use of synthetic oil as heat transfer fluid. However, it is necessary to assess if this operating temperature also maximizes the electrical power production during situations of low levels of incident solar radiations, such as the passage of clouds (Paper 1).

- *The solution to the problem of the appearance of temperature peaks.* This problem appears in some loops of the field during the passage of clouds when the field is controlled by the commercial control strategies. When a cloud is passing over the field, it covers some of its loops, and therefore the outlet oil temperature controller has to lower the oil flow to reject that disturbance. Nevertheless, the drop of the oil flow in the loops not covered by the cloud may lead to an increase in the outlet oil temperature. If the temperature reaches its security limit the collectors are programmed to get out of focus to prevent oil degradation, leading to a loss of power. This problem is solved by the use of a MPC with nonlinear constraints (Congress Paper).

- *The development and assessment of a new control strategy based on a MPC that can allow a real time optimization of the electrical power.* The objective is to maximize the electrical power produced by the solar plant in real time, depending on the value of the incident solar radiation. The prediction of the future clouds is taken into account in the MPC algorithm (Paper 2).

- *The development and assessment of a new control strategy based on a MPC to apply to solar thermal plants with thermal storage system.* In this case the objective is to maximize the thermal energy stored while keeping the electrical power production at its reference value. With this new objective it is possible to increase the number of hours that the plant can provide the electrical power demanded when there is no solar radiation (Paper 3).

Chapter 3

Results and Discussion

The results obtained in this thesis can be divided into three different groups, each related to one of the three stages of study described in Chapter 1. The first one includes the results of the study of the optimum operating temperature of the solar collector field. This study was carried out using steady state models of the solar field and the power cycle, and was aimed to determine how the outlet oil temperature of the field have to change according to the value of the solar radiation in order to maximize the electrical power produced. One of the simulations done in this study shows how the outlet oil temperature of the field has to change during the start and the end of the day, and also when there are clouds passing through the field (figure 3.1). Therefore, it seems that it was necessary to develop a control strategy that can make a real time optimization of the operating temperature instead of continue using control strategies whose aim is to keep constant the value of this temperature around the maximum allowable one (400°). The complete description of the models used and the simulation results as well as the discussion of these results can be found in Paper 1.

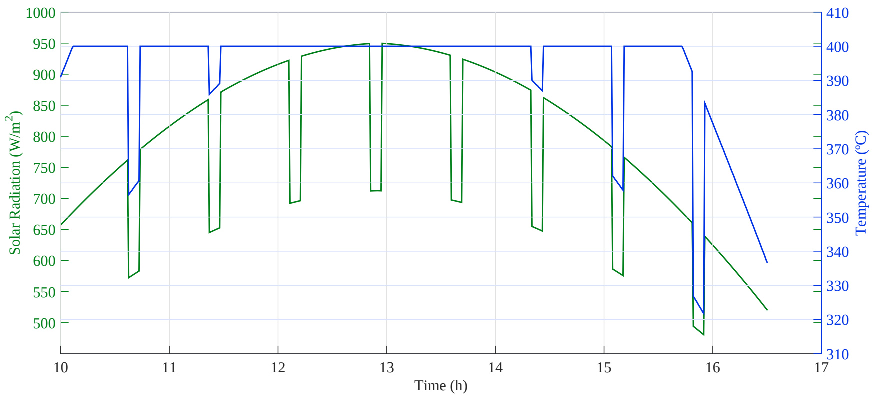

Figure 3.1: Change of the optimum temperature during a cloudy day

In the second stage of the study the aim was to develop an optimal control strategy that maximizes the electrical power produced. The first idea was to use a static optimizer that calculates the optimum operating temperature and then send it as the set point value to a PI controller followed by a series feedforward. However, due to the sudden and quick changes produced by the passage of the clouds in the level of incident solar radiation that reaches the field a static optimizer is not accurate enough. For that reason a real time optimizer was selected instead. This optimizer consisted of a MPC that used predictions of the passage of the clouds to calculate the optimum oil flow that maximizes the electrical power produced. The use of the oil flow instead of the outlet oil temperature is due to the fact that for a specific value of the incident solar radiation and the oil flow, the value of the outlet oil temperature is set (they are dependent variables). This MPC was implemented on the solar plant simulator with two different configurations; one in which the MPC manipulates the total oil flow and then it is divided equally among the loops (GS), and another one in which the MPC manipulates individually the oil flow circulating through each loop (DS). Both configurations were assessed and compared to a control strategy that keeps constant the outlet oil temperature.

In figure 3.2 it can be seen the electrical power produced by the constant temperature strategy and both MPC configurations during days with different time of passage of clouds covering the field. The time of passage is defined as the number of integration steps there are no clouds passing over the field between the moment the last cloud left the field and a new one comes in. It is clear that the MPC strategies achieve a higher production of electrical power in all cases compared to the constant temperature strategy;

in addition, the higher the presence of passing clouds during the day, which means a low time of passage, the higher the percentage of improvement in power production achieved. In Paper 2 this study it is explained in detail.

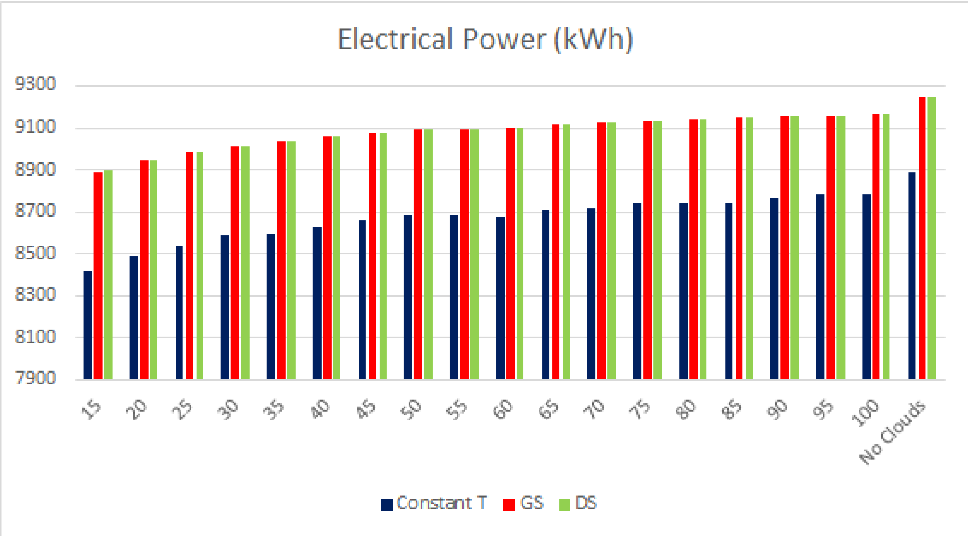

Figure 3.2: Electrical power generated for different pass frequencies of the clouds, by the global (GS) and distributed (DS) strategies and a control strategy which tries to keep constant the oil outlet temperature at 390°C

Finally, the third group consists of the results obtained by applying a real time optimization to a solar plant with a thermal storage system. The aim of this optimization is to maximize the thermal energy stored while keeping the electrical power produced at its demanded value. For that reason, a MPC similar to the one described before was used. Nevertheless, in this case the objective function was changed according to the new optimization aim, and the configuration used was the one in which the MPC manipulates the total oil flow and then it is divided equally among the loops. The performance of this MPC was compared to a control strategy that consisted of a PI followed by a feedforward to control the outlet temperature of the field (at a constant value around the maximum allowable one) and another PI to control the electrical power manipulating the oil mass flow sent to the storage system and therefore, the oil mass flow sent to the power cycle (the total oil mass flow is the addition of these two flows). In figures 3.3 and 3.4 it is shown how the MPC achieves a better control of the electrical power and a higher amount of stored thermal energy (a higher oil mass flow sent to the storage system implies a higher amount of molten salts stored in the hot tank, that in turns, increases the number of operation hours of the plant when there is no solar radiation). The results obtained with this control strategy are completely discussed in Paper 3. ,

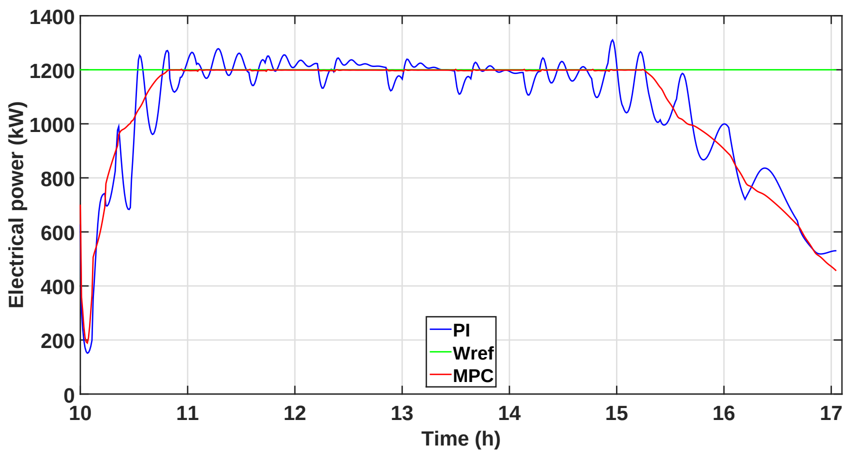

Figure 3.3: Electrical power generated by the constant temperature and MPC strategies

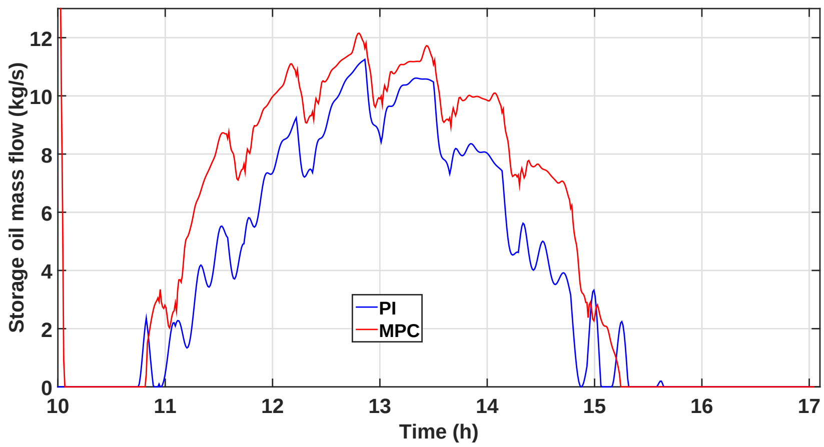

Figure 3.4: Storage oil mass flow with the constant temperature and MPC strategies

Chapter 4

Conclusions

The studies carried out during the development of this thesis have resulted in a set of conclusions that can be divided into four different groups:

- The study made in Paper 1 shows that in order to maximize the electrical power produced by the solar field, it is necessary to calculate the optimum operating temperature associated to each value of the incident solar radiation; for that reason in that paper was proposed a methodology to calculate that optimum. It was also demonstrated that at high values of the incident solar radiation the optimum operating temperature is the highest allowable one, which is the value of temperature used in commercial plants for the entire operation. However, at low values of the incident solar radiation the optimum temperature is lower than the highest allowable one, being the improvement in the electrical power produced by using this optimum temperature instead of the highest one up to a 4%.

- The use of the control strategy that keeps constant the oil outlet temperature of the field may lead to the appearance of the temperature peaks problem, described in the Congress Paper, and with that strategy the only way to avoid this problem is to lower the temperature set point, resulting in a loss in the electrical power production. Nevertheless, the optimal control strategy proposed in that paper (based on a MPC) not only solve the problem of the temperature peaks, but also maximizes the electrical power production.

- In Paper 2 two MPC configurations were assessed and compared to a control strategy that keeps constant the oil outlet temperature of the field. There were two main conclusions in that paper, the first one is that the use of any of the MPC configurations achieves an improvement in the electrical power between 4% and 5.7% depending on the level of coverage of the field due to the passage of clouds. According to the first group of conclusions the 4% improvement corresponds to a clear day, and therefore the improvement associated with the presence of clouds covering the field would be up to 1.7%. The second one is that the MPC configuration that manipulates individually the oil flow circulating through each loop achieves a negligible improvement compared to the configuration that manipulates the total oil flow that then is equally divided among the loops.

- The MPC proposed in Paper 3 for solar plants with a thermal storage system was compared to a commercial control strategy that operates the field at a constant value of the oil outlet temperature. Although the results obtained for different situations related to the passage of the clouds are different from each other, two main conclusions can be drawn. The first one is that the time of electrical power production achieved by the MPC is around 12% (the mean result between the different situations simulated) higher than the one obtained with the commercial strategy. The second one is that with the MPC a better controllability of the electrical power produced is achieved, resulting in a monetary gain because of the smaller deviation from its demanded value, which is usually penalized.

Chapter 5

Paper 1

Optimum Operating Temperature of Parabolic Trough Solar Fields
Sergio J. Navas, Pedro Ollero, and Francisco R. Rubio. Solar Energy. Volume 158, 2017. DOI:https://doi.org/10.1016/j.solener.2017.09.022

This paper shows the relationship between the incident solar radiation and the optimum outlet temperature of a solar field to produce the highest amount of electrical power. Various simulations were made for different values of incident solar radiation, calculating for each one the optimum temperature which produces the maximum electrical power and demonstrating that to operate the field at the highest allowable temperature is not the optimal operating point from certain values of solar radiation; a situation which takes special relevance during cloudy days. These simulations were carried out using two connected models, one for the solar field and another one for the power cycle.

5.1 INTRODUCTION

The main technologies for converting solar energy into electricity are photovoltaic (PV) and concentrated solar thermal (CST). Parabolic trough, solar towers, Fresnel collector and solar dishes are the main technologies used for concentrating solar energy. This paper focuses on parabolic trough solar thermal power plants, which consist of a collector field (Fig.5.1), a power cycle, a thermal energy storage (TES), and auxiliary elements such as pumps, pipes and valves. The solar collector field collects solar radiation and focuses it onto a tube in which a heat transfer fluid, usually synthetic oil, circulates. The heat gained by the oil is used by the power cycle to produce electricity by means of a steam turbine. Another way to produce the steam needed by the turbine is the direct steam generation (DSG), a type of CST plant where the steam is produced directly in the pipes.

The main goal of a parabolic trough solar field is to collect the maximum solar energy in order to produce as much electrical power as possible. Normally, this is achieved by keeping the outlet temperature of the field around the maximum allowable value, that is 400°C, due to oil degradation. However, in this paper, we will prove that this way to operate the field does not produce the best results of electrical power generated. That is due to the fact that the electrical power depends on both the oil flow and temperature, in such way, that when the value of solar radiation is low, to operate at a maximum temperature would imply that the oil flow would be so small that the electrical power generated would not be the maximum possible. This problem has been studied before in [15], where it was suggested that the optimum strategy is based on adapting the oil outlet temperature to the incident solar radiation, keeping constant the superheating temperature of the steam; it was also studied in [18] where a constant outlet temperature was used (393°C). Finally, a more recent study was carried out in [7] where it was proposed to change the outlet temperature set point according to the value of the solar radiation. The set point is calculated by an optimizer and then is tracked with a series feedforward with a PID controller.

The main novelty of this paper is that the effect of the solar radiation on the optimal outlet temperature was studied with a complete power cycle model rather than only using a formula that only depends on the oil outlet temperature and not taking into account the oil mass flow for calculating the electrical power; which was the case of [7]. In [16] a complete power cycle model it is also used, but its application is to predict the off-design performance of parabolic trough solar plants, instead of using it to calculate the optimum temperature, which is the case of the paper presented here. The calculations obtained with this power cycle model, in spite of its simplicity, agree with the ones found in the literature [13]-[15], that it is not the case of the results shown in [7]. In addition the simulations made in this paper were not focused on studying particular working days, that is the case of [15] and [7] but on determining for different values of solar radiation what the optimum value of outlet temperature should be; something that is specially useful during cloudy days. The models used in this paper were developed to be used also in control purposes by making little changes, like adapting the parameters of the field and power cycle to match those of the target field, and adding dynamic to the power cycle. This dynamic can be assumed to be the same that of the boiler, which is the slowest one of the power cycle.

Using the software Engineering Equation Solver©, the authors have simulated a parabolic trough solar field connected with a power cycle. These simulations have been carried out for different values of solar radiation, calculating for each one the optimum value of outlet temperature which produces the highest amount of electrical power. This optimum value also corresponds to the optimum value of oil flow, due to the fact that both variables are dependent for a given value of I. The power cycle used in this paper is a Rankine cycle with a maximum temperature of 374°C, a maximum pressure of 70,5 bar, and a power range of 800-2330 kW. The selection of a Rankine cycle is due to the fact that it is the same used in the ACUREX field, however, the power range has been increased according to the size increase made to the field used in this paper, and the working temperature has been increased to match those used by the commercial plants.

The paper is organized as follows: Section 2 describes the model of the solar field used for simulation purposes. Section 3 describes the model of the power cycle. Section 4 shows the results obtained by simulations of the solar field connected with the power cycle (Fig.5.2). Finally, the paper draws to a close with some concluding remarks.

Figure 5.1: ACUREX distributed solar collector field

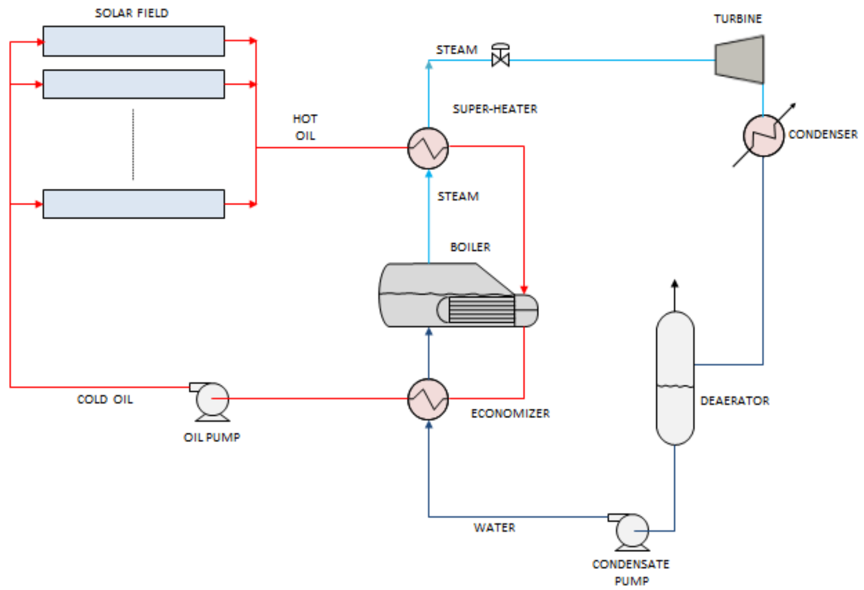

Figure 5.2: Diagram of the solar field connected with the power cycle

5.2 SOLAR FIELD MODEL

In this section, the mathematical model of a parabolic trough is presented. This model is the same used in [19] which is at the same time a modification (mainly the modeling of all field loops, instead of modeling only one of its loops and supposing the behavior of the entire field to be the same) of the model proposed by [3]-[6]-[8] for the ACUREX field (Fig. 5.1). Basically, this model can be used to simulate parabolic trough solar fields by selecting parameters like the number of active (the parts where the solar radiation reaches the tube) and passive (joints and other parts not reached by concentrated solar radiation) zones, length of each zone, or collector aperture. The solar field simulated in this paper is supposed to be on the site of the Escuela Superior de Ingeniería de Sevilla. The field consists of 3456 distributed solar collectors. These collectors are arranged in 48 rows (being 3 meters the row spacing between parallel collectors) which form 24 parallel loops (each of the loops is 480 meters long), each one with 8 modules of 18 collectors. The collectors have dimensions of 3x1.82 meters and their factory is EuroTrough. Each loop is modeled by the following system of partial differential equations describing the energy balance:

Active zones

$$\rho_m C_m A_m \frac{\partial T_m}{\partial t} = I n_0 G - H_l G (T_m - T_a) - d H_t (T_m - T_f) \tag{5.1}$$

Fluid element

$$\rho_f C_f A_f \frac{\partial T_f}{\partial t} + \rho_f C_f \dot{q} \frac{\partial T_f}{\partial x} = d H_t (T_m - T_f) \tag{5.2}$$

Passive zones

$$\rho_m C_m A_m \frac{\partial T_m}{\partial t} = -G H_p (T_m - T_a) - d H_t (T_m - T_f) \tag{5.3}$$

where the sub-index m refers to metal and f refers to the fluid. The model parameters and their units are shown in Table 5.1.

Table 5.1: Solar field model parameters and variables description

Symbol	Description	Units
t	Time	s
x	Space	m
ρ	Density	kg/m^3
C	Specific heat capacity	J/(K kg)
A	Cross sectional area	m^2
T	Temperature	°C
$\dot{q}$	Oil flow rate	m^3/s
I	Solar radiation	W/m^2
n_0	Optical efficiency	Unit-less
G	Collector aperture	m
T_a	Ambient Temperature	°C
H_l	Global coefficient of thermal losses for active zones	W/(m^2 °C)
H_t	Coefficient of heat transmission metal-fluid	W/(m^2 °C)
H_p	Global coefficient of thermal losses for passive zones	W/(m^2 °C)
d	Pipe diameter	m

The density ρ and specific heat C depend on fluid temperature [3], being the thermal fluid used Santotherm 55. The coefficient of heat transmission H_t depends on temperature and oil flow [3]. The incident solar radiation I depends on hourly angle, solar hour, declination, Julianne day, and local latitude [3]-[6]-[8]. The pipe has a length of 480 m and a cross sectional area of $5.3 * 10^{-4}$ m^2. The collector aperture is 1.82 m and the optical efficiency is 0.675 [3]-[7]. The coefficient of thermal losses for active zones H_l and for passive zones H_p has a value of 0.49 and 0.24 W/(m^2 °C) respectively [3]-[6]-[8]. These values have been assumed to be constant as in [16]. In order to solve this system of partial differential equations, a two stage finite difference equation has been programmed, considering each segment of 1 m for the passive zones and of 3 m for the active zones and solving (5.1)-(5.2)-(5.3).

This solar field model is connected with a power cycle model (Fig.5.2) as commented in section 1. Both have to be simulated at the same time because some of their parameters are shared. Specifically, to simulate the field, the value of the inlet temperature is needed and it can only be obtained after solving the equations of the cycle model. At the same time, to simulate the cycle, the outlet temperature and the oil flow are needed. Therefore, the simulation of both models is an iterative process.

5.3 POWER CYCLE MODEL

The power cycle simulated in this paper consists of an economizer, a boiler and a super-heater (each one denoted by the subscript E, B and S respectively) followed by a turbine. The model we use is a steady state model because the aim of the study is not to test it during an operating day, but to show what value the optimal temperature should have depending on the value of the incident solar radiation.

Following the way traveled by the oil flow, firstly it enters into the super-heater where the steam flow is overheated to a certain temperature. This super-heater was modeled by equations (5.4), which form a system of three equations and three unknown values. The unknown values are the outlet oil and outlet steam temperatures, T_{oo} and T_{os} respectively, and the heat exchanged in the super-heater Q_S. The heat exchangers (E, B and S) have been designed following the typical rule that the temperature difference at the outlet of each heat exchanger for the nominal operating point (900W/m^2 of solar radiation and 393°C of oil outlet temperature) was 10°C [17].This has allowed the values of the thermal transmittance U and the exchange area A of each exchanger to be set (table 5.2). Then the supposition that this value will be constant was made, assuming the associated errors. The specific heat of both, the oil C_{Po} and the steam C_{Ps} depend on fluid temperature, being the first one calculated by the correlation in [3] and the second one using the steam property tables. The mass flow m_o and inlet temperature T_{io} of the oil were given by the solar field model and the mass flow m_s and inlet temperature T_{is} of the steam were given by the boiler model that will be shown below. Finally, the logarithmic mean temperature difference $LMTD$ needed in one of the equations was calculated using equation (5.7). See Table 5.3 for a more detailed description of the power cycle variables and parameters.

Table 5.2: Values of UA

Parameter	Value (kJ/s °C)
$U_S A_S$	20.15
$U_B A_B$	96.95
$U_E A_E$	25

$$\begin{aligned} m_o C_{Po} T_{io} - Q_S &= m_o C_{Po} T_{oo} \\ m_s C_{Ps} T_{is} + Q_S &= m_s C_{Ps} T_{os} \\ Q_S &= U_S A_S LMTD_S \end{aligned} \tag{5.4}$$

After the super-heater, the oil flow is used to boil the water flow to produce saturated steam. This process is carried out at a floating pressure to maximize the amount of heat exchanged. Equations (5.5) are used to model the boiler. Again, these equations form a system of three equations and three unknown values, which are the outlet oil and outlet steam temperatures, T_{oo} and T_{os} respectively and the heat exchanged in the boiler Q_B. Due to the fact that this is a steady state model, the water flow m_w is equal to the steam flow m_s. The heat of vaporization H_v can be found in the steam tables. The rest of variables can be obtained in the same way than in the paragraph before. The liquid level is assumed to be constant. This assumption is correct if this level is going to be controlled by fast controller.

$$\begin{aligned} m_o C_{Po} T_{io} - Q_B &= m_o C_{Po} T_{oo} \\ m_w C_{Pw} T_{iw} + Q_B &= m_s H_v + m_w C_{Pw} T_{os} \\ Q_B &= U_B A_B LMTD_B \end{aligned} \tag{5.5}$$

Finally, the oil flow is introduced into an economizer where it is used to preheat the water flow, and then it is recycled to the field. The economizer was modeled by equations (5.6). In this case, as with the previous ones, we have a system of three equations and three unknown values, which are the outlet oil and outlet water temperatures, T_{oo} and T_{ow} respectively and the heat exchanged in the economizer Q_E. The other variables are calculated as explained in the super-heater.

$$\begin{aligned} m_o C_{Po} T_{io} - Q_E &= m_o C_{Po} T_{oo} \\ m_w C_{Pw} T_{iw} + Q_E &= m_w C_{Pw} T_{ow} \\ Q_E &= U_E A_E LMTD_E \end{aligned} \tag{5.6}$$

$$LMTD = \frac{(T_{io} - T_{os}) - (T_{oo} - T_{is})}{\ln\left(\frac{(T_{io}-T_{os})}{(T_{oo}-T_{is})}\right)} \tag{5.7}$$

The steam flow generated in the super-heater is then introduced into a high pressure turbine. In order to model this turbine we used the Willan's Line Method described in [23]. Firstly, the turbine's outlet pressure is set at a value of 5.63 kPa, which is a typical value for condensation turbines, because it allows the use of water at ambient temperature to condensate the steam. Then, to calculate inlet pressure equation (5.8) is used, which is a modification of the Stodola equation [24] when the inlet pressure is far higher than the outlet one, as it is the case. With these pressure values it is possible to calculate the saturation temperature of the inlet and the outlet steam flow, so that, the difference of saturation temperature ΔT_s could be known and therefore used in equations (5.9) to calculate parameters a and b if the generated power by the turbine is lower or equal than 2000 kW, and in equations (5.10) if it is higher than 2000 kW.

$$P_i = k m_s \tag{5.8}$$

$$\begin{aligned} a &= 0.66 \Delta T_s \\ b &= 1.19 + 7.59 * 10^{-4} \Delta T_s \end{aligned} \tag{5.9}$$

$$\begin{aligned} a &= -463 + 3.53 \Delta T_s \\ b &= 1.22 + 1.48 * 10^{-4} \Delta T_s \end{aligned} \tag{5.10}$$

After that, it is necessary to calculate the isentropic difference of enthalpy ΔH_i and to set the parameter L which is the interception rate and depends on the turbine characteristics, being its typical value between 0.05 and 2. With these two parameters and with a and b we can calculate n and W_{int} using equations (5.11) and with them, using equation (5.12) we can calculate the electrical power generated by the turbine.

$$\begin{aligned} n &= \frac{(L+1)}{b}(\Delta H_i - a/m_s) \\ W_{int} &= \frac{L}{b}(\Delta H_i m_s - a) \end{aligned} \tag{5.11}$$

$$W = nm_s - W_{int} \tag{5.12}$$

The net electrical power produced by the field is the result of subtracting the power consumed by the pump to the power generated by the turbine. Therefore, to calculate the consumption of the pump we used the Darcy equation (5.13). The Reynolds number and the Barr's friction coefficient needed in the equation (5.13) are computed by (5.14) and (5.15) respectively:

$$hpl = 9806.65\frac{8fl\dot{q}^2}{g\pi^2 d^5} \tag{5.13}$$

$$Re = \frac{\rho_f \dot{q} d}{A_f \mu} \tag{5.14}$$

$$f = 0.25\frac{1}{(log10(\frac{\epsilon_r}{3.7d} + \frac{5.74}{Re^{0.9}}))^2} \tag{5.15}$$

The power consumption depends on the pump efficiency , oil flow and the pressure drop hpl (5.16).

$$W_{pump} = \frac{hpl}{\eta_{pump}}(W) \tag{5.16}$$

Finally, the net electrical power is calculated by (5.17) and the cycle efficiency with (5.18).

$$W_{net} = W - W_{pump}(kW) \tag{5.17}$$

$$\eta = \frac{W_{net}}{Q_S + Q_B + Q_E} \tag{5.18}$$

A summary of the model parameters and their units are shown in Table 5.3.

Table 5.3: Power cycle model parameters and variables description

Symbol	Description	Units
Q	Exchanged heat	kW
m	Mass flow	kg/s
C	Specific heat capacity	kJ/(K kg)
A	Exchange area	m^2
T	Temperature	°C
U	Thermal transmittance	kW/(m^2 °C)
$LMTD$	Logarithmic mean temperature difference	°C
H	Enthalpy	kJ/kg
P	Pressure	kPa
a	Correlating parameter for steam turbines	kW
b	Correlating parameter for steam turbines	Unit-less
L	Interception rate	Unit-less
n	Slope of the Willans' Line	kW/kg
W_{int}	Willans' Line intercept	kW
η	Power cycle efficiency	Unit-less
ρ_f	Fluid density	Kg/m^3
$\dot{q}$	Oil flow	m^3/s
A_f	Cross sectional area	m^2
μ	Dynamic viscosity	Kg/(m s)
d	Pipe diameter	m
ϵ_r	Relative rugosity	m
g	Gravity	m/s^2
l	Loop length	m
pd	Pressure drop	Pa

5.4 SIMULATION RESULTS AND DISCUSSION

This section of the paper shows the results obtained by simulations made with the models described in the previous sections. The aim of these simulations is to determine from which value of solar radiation it is better to operate the field at lower temperature than the maximum allowable and higher oil flow rather than at maximum temperature and lower oil flow. Therefore, these simulations were carried out calculating the optimum outlet temperature for each value of solar radiation. The maximum allowed value of outlet temperature is 400 °C to prevent oil degradation, and the oil mass flow is bounded between 3.7 and 37 kg/s according to the minimum and maximum allowed velocity through pipes (0.5-5 m/s). The procedure for obtaining the optimum operating temperature may be summarized as follows:

- The optimizer selects a value for the independent variable, which is the oil flow $\dot{q}$.

- After the value of the oil flow is selected, the collector field model (equations (5.1)-(5.2)-(5.3)) is used to calculate the outlet oil temperature of the field.

- With the values of the oil outlet temperature and the oil flow, equations (5.4)-(5.5)-(5.6)-(5.7) are used to obtain the mass flow and the temperature of the steam produced and the oil temperature returning to the field T_{in}.

- The values of mass flow and temperature of the steam are used in order to solve equations (5.8)-(5.9)-(5.10)-(5.11)-(5.12)and in doing so, obtaining the value of the electrical power generated by the turbine W.

- With equations (5.14)-(5.15)-(5.13)-(5.16)-(5.17) and the previous value of W, the net electrical power W_{net} is calculated.

- All the items explained before will be repeated until the optimizer reaches the value of oil flow that results in the maximum value of the net electrical power W_{net}.

The value of the variables at the nominal conditions is shown in Table 5.4

Table 5.4: Solar field and power cycle at nominal conditions

Variable	Value	Units
$T_{in}field$	264.3	°C
$T_{out}field$	390	°C
m_{oil}	22.2	kg/s
m_{steam}	2.94	kg/s
$T_{in}turbine$	373.9	°C
$P_{in}turbine$	7050	kPa
P_{cond} (35°C)	5.63	kPa
$W(gross)$	2330	kW
W_{pump}	61.24	kW
W_{net}	2268	kW
η	26.66	%

In figures 5.3(a) and 5.3(b) it can be seen how the electrical power and the efficiency decrease while the solar radiation does, but the optimum value of the temperature is kept constant at its maximum allowed value until certain value of solar radiation, from which it starts to decrease. Note that, despite the simplicity of our cycle model, the efficiency values are close to the real ones for a small field [13]. Accordingly, figures 5.4(a) and 5.4(b) show for the same situation, how the oil flow has to decrease to maintain a constant value of the temperature until the solar radiation reaches the same value commented before, from which the oil flow starts to increase in order to lower the value of the temperature.

The breaking point shown in figures 5.3 and 5.4 happens when the calculated value of the optimum temperature is lower than the maximum allowable one, which is 400C. Until that point is reached, this maximum temperature constraint is active and that is the reason for the appearance of the breaking point. Between 650W/m2 to 900 W/m2 the oil flow is decreasing in order to achieve the optimum value of the outlet temperature, which is for that value of solar radiation, the maximum one. For lower values of solar radiation the optimum temperature decreases and so, the oil flow has to increase. However, the electrical power generated continually decreases according to the decreasing value of the incident solar radiation, with a change in the slope when the breaking point of the temperature and oil flows happens.

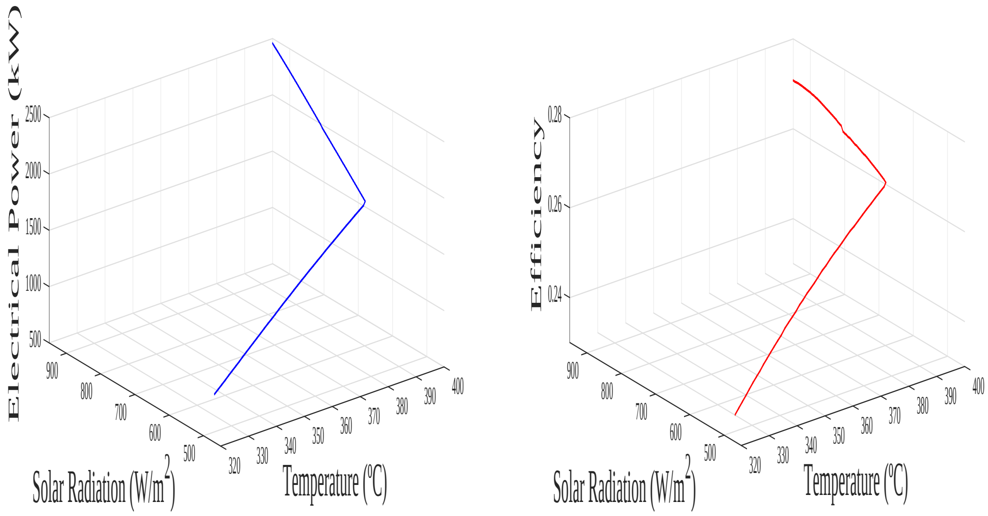

(a) Electrical power (b) Cycle efficiency

Figure 5.3: Electrical power and cycle efficiency as a function of the temperature

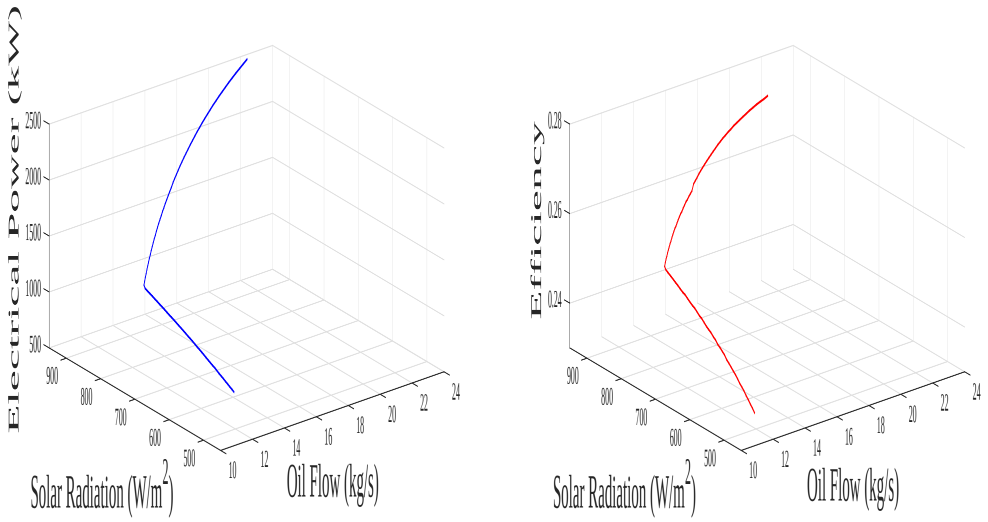

(a) Electrical power (b) Cycle efficiency

Figure 5.4: Electrical power and cycle efficiency as a function of the oil flow

In addition, figure 5.5 shows how the operating temperature should change during a clear day, whereas in figure 5.6 it is presented the case of a cloudy one. In this final case it is clear that depending on the number of clouds and the total amount of field covered we will have to change the operating point many times during the day to get the maximum amount of electrical power. For that reason, figure 5.7 shows the percentage of improvement achieved by operating at the optimum temperature instead of keeping it constant at its maximum allowable value, to demonstrate how much favorable it could be; specially at low levels of solar radiation.

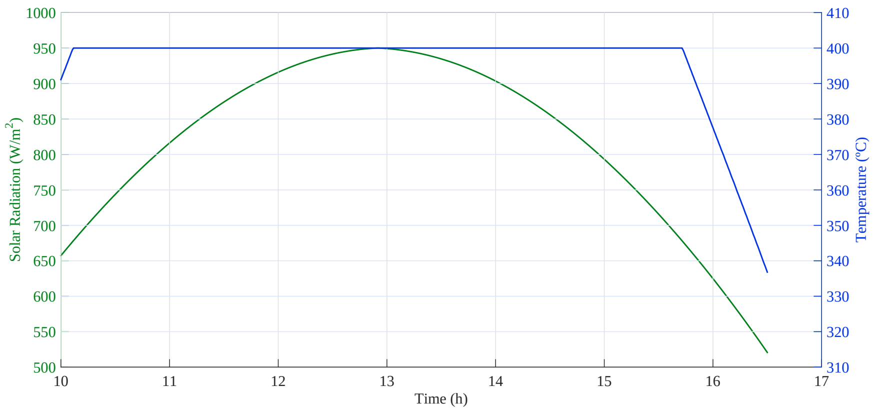

Figure 5.5: Change of the optimum temperature during a clear day

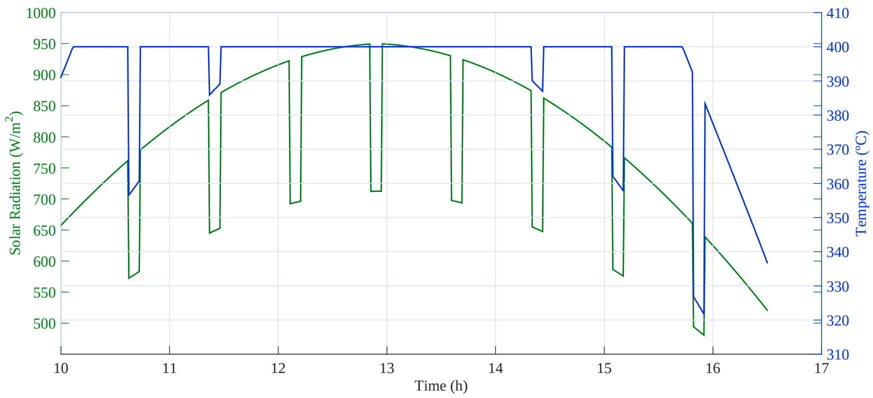

Figure 5.6: Change of the optimum temperature during a cloudy day

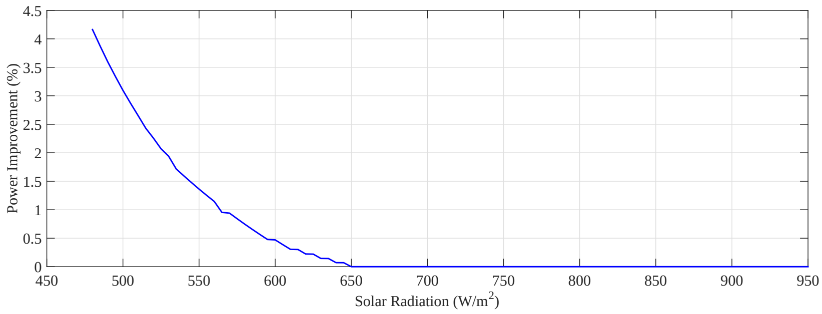

Figure 5.7: Percentage of improvement achieved by operating at optimum temperature rather than at the maximum allowable one

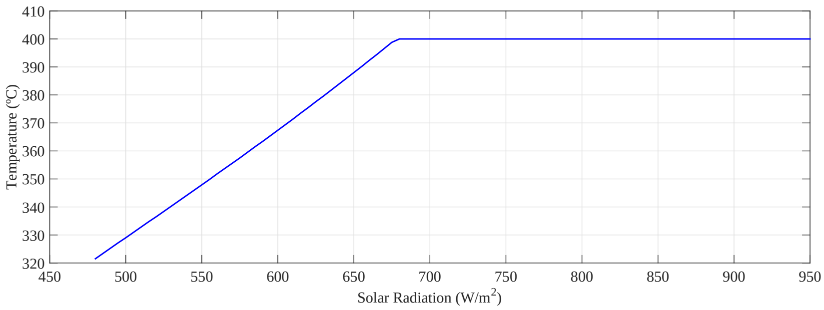

(a) Temperature

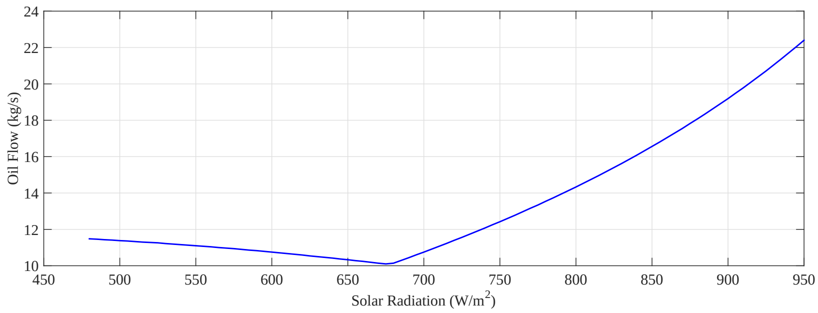

(b) Oil flow

Figure 5.8: Optimum temperature and oil flow depending on solar radiation

Finally in figures 5.8(a) and 5.8(b) it can be seen in a clearer way where the change of trend in both temperature and oil flow is produced. Seeing these figures, it is clear that for solar radiation values higher than around 670 W/m2, to operate the field at the maximum allowable temperature produces the higher value of electrical power. However, from that value of radiation to lower ones it can be seen that it is better to reduce the outlet temperature and consequently to increase the oil flow. These results are contrary to the ones shown in [18] where a constant outlet temperature is used, and in [15], where it was suggested that the optimum strategy is based on adapting the fluid outlet temperature to the incident solar radiation, keeping constant the superheating temperature of the steam. However, compared to the results obtained in [7] the conclusions are similar, but the values of the efficiency of the power cycle and the improvement achieved are far higher than the obtained in this paper and in the previously mentioned. This is due to the simplification the authors made by assuming that the cycle efficiency only depends on the outlet oil temperature. Therefore, we can prove what was discussed previously in the introduction.

5.5 CONCLUSIONS

The main conclusion of this paper is that the optimum outlet temperature to operate a parabolic trough solar field depends on the value of incident solar radiation, and so a methodology for calculating that optimum value is needed, especially when its value is low due to the passage of clouds.

In most cases the solar field will operate at high levels of radiation, which implies that maximum values of outlet temperature will be the optimum ones. Therefore, the results obtained by this study take relevance in days with partial coverage due to the effect of clouds passing over the field and at the beginning and end of the day. In these cases it is better to lower the outlet temperature by increasing the oil flow when the cloud is passing, but then, when it leaves the field, it is necessary to get back to the previous values of outlet temperature and oil flow.

Bibliography

[1] Abutayeh, M., Alazzam, A. and El-Khasawneh, B. (2014). *Balancing heat transfer fluid flow in solar fields.* Solar Energy, 105, 381-389.

[2] Barão, M., Lemos, J. and Silva, R. (2002). *Reduced complexity adaptive nonlinear control of a distributed collector solar field.* Journal of Process Control, 12-1, 131-141.

[3] Camacho, E. F., Berenguel, M. and Rubio, F. R. (1997). *Advanced control of solar plants, first ed.* Springer-Verlag, London.

[4] Camacho, E. F., Rubio, F. R., Berenguel, M. and Valenzuela, L. (2007). *A survey on control schemes for distributed solar collector fields. Part I: Modeling and basic control approaches.* Solar Energy, 81-10, 1240-1251.

[5] Camacho, E. F., Rubio, F. R., Berenguel, M. and Valenzuela, L. (2007). *A survey on control schemes for distributed solar collector fields. Part II: Advanced control approaches.* Solar Energy, 81-10, 1252-1272.

[6] Camacho, E. F., Berenguel, M., Rubio, F. R. and Martínez, D. (2012). *Control of solar energy systems, first ed.* Springer-Verlag, London.

[7] Camacho, E. F. and Gallego, A. (2013). *Optimal operation in solar trough plants: A case study.* Solar Energy, 95, 106-117.

[8] Carmona, R., (1985). *Análisis, modelado y control de un campo de colectores solares distribuidos con sistema de seguimiento en eje.* Ph.D. Thesis. Universidad de Sevilla.

[9] Cirre, C., Berenguel, M., Valenzuela, L. and Camacho, E. F. (2007). *Feedback linearization control for a distributed solar collector field.* Control Engineering Practice, 15-12, 1533-1544.

[10] CIRRE, C., BERENGUEL, M., VALENZUELA, L. and KLEMPOUS, R. (2009). *Reference governor optimization and control of a distributed solar collector field.* European Journal of Operational Research, 193, 709-717.

[11] COLMENAR-SANTOS, A., MUNUERA-PREZ, F., TAWFIK, M. and CASTRO-GIL, M. (2014). *A simple method for studying the effect of scattering of the performance parameters of parabolic trough collectors on the control of a solar field.* Solar Energy, 99, 215-230.

[12] GALLEGO, A. and CAMACHO, E. F. (2012). *Estimation of effective solar irradiation using an unscented kalman filter in a parabolic-trough field.* Solar Energy, 86-12, 3512-3518.

[13] GARCÍA, S. (2012). *Guía técnica de la energía solar termoeléctrica* Fenercom, Capítulo 1.<www.fenercom.com/pdf/publicaciones/Guia-tecnica-de-la-energia-solar-termoelectrica-fenercom-2012.pdf>

[14] LIMA, D., NORMEY-RICO, J. and SANTOS, T. (2016). *Temperature control in a solar collector field using filtered dynamic matrix control.* ISA Transactions, 62, 39-49.

[15] LIPPKE, F. (1995). *Simulation of the part-load behavior of a 30 MWe SEGS plant.* Report No. SAND95-1293, SNL, Albuquerque, NM, USA.

[16] MANZOLINI, G., GIOSTRI, A., SACCILOTTO, C., SILVA, P. and MACCHI, E. (2012). *A numerical model for off-design performance prediction of parabolic trough based solar power plants.* Journal of Solar Energy Engineering, Vol.134.

[17] MARCH, L. (1998). *Introduction to pinch technology* Targeting House, Gadbrook Park, Northwich, Cheshire, CW9 7UZ, England.

[18] MONTES, M., ABÁNADES, A., MARTÍNEZ-VAL, J. and VALDÉS, M. (2009). *Solar multiple optimization for a solar-only thermal power plant, using oil as heat transfer fluid in the parabolic trough collectors.* Solar Energy, 83-12, 2165-2176.

[19] NAVAS, S. J., RUBIO, F. R., OLLERO, P. and ORTEGA, M. G. (2016). *Modeling and simulation of parabolic trough solar fields with partial radiation.* XV European Control Conference, 31-36.

[20] PRICE, H., LUPFERT, E., KEARNEY, D., ZARZA, E., COHEN, G., GEE, R. and MAHONEY, R. (2002). *Advances in parabolic trough solar power technology.* Journal of Solar Energy Engineering, 124-2, 109-125.

[21] Rubio, F. R., Camacho, E. F. and Berenguel, M. (2014). *Control de campos de colectores solares.* Ibero-American Journal of Industrial Automation and Informatics (RIAI), 3-4, 26-45.

[22] Shinskey, F. (1978). *Energy conservation through control.* Academic Press.

[23] Smith, R. (2005). *Chemical process design and integration.* Wiley.

[24] Stodola, A. (1945). *Steam and gas turbines.* Vol. 1, Peter Smith, New York.

Chapter 6

Paper 2

Optimal Control Applied to Distributed Solar Collector Fields with Partial Radiation
Sergio J. Navas, Francisco R. Rubio, Pedro Ollero, and João M. Lemos. Solar Energy. Volume 159, 2018. DOI:https://doi.org/10.1016/j.solener.2017.11.052

This paper describes and assesses two strategies to control distributed solar collector fields, especially during days with partial radiation due to the passage of clouds. The main objective of these control strategies is to maximize the electrical power generated during different situations in which different parts of the solar field receive different degrees of solar radiation. Simulations were carried out using two connected models, one for the solar field (taking into account all of its loops), that includes the passage of clouds, and another one for the power cycle. The solar field simulated is a pilot plant, in which it is assumed that all the loops have the same characteristics; and the nominal power range of the Rankine cycle is 800-2330kW. Finally, the improvement in electrical power achieved by both strategies is compared with a typical control strategy that tries to keep constant the outlet oil temperature of the field. This improvement varies between 4% for clear days and 5.7% for cloudy days.

6.1 INTRODUCTION

The main technologies for converting solar energy into electricity are photovoltaic (PV) and concentrated solar power (CSP). Parabolic trough, solar towers, Fresnel collector, and solar dishes are the most used technologies for concentrating solar energy. This paper focuses on parabolic trough solar fields, that consist of a collector field (Fig. 6.1), a power cycle, and auxiliary elements such as pumps, pipes, and valves. The solar collector field collects solar radiation and focuses it onto a tube in which a heat transfer fluid, such as synthetic oil, circulates. The oil is heated up and then used by the power cycle to produce high pressure steam in a boiler, and electricity by expanding it in a turbo-generator.

Figure 6.1: ACUREX distributed solar collector field

The main goal of a parabolic trough solar field is to collect solar energy in order to produce as much electrical power as possible. Normally, most of the solar thermal power plants try to achieve this objective by keeping the outlet oil temperature of the field around the maximum allowable value, that in this case is 400°C, imposed to prevent oil degradation. However, some studies like [15] and [7] show that this way to operate the field does not produce the best results of electrical power generated. In [15] it was suggested that the optimum strategy is based on adapting the oil outlet temperature to the incident solar radiation, keeping constant the superheating temperature of the steam, whereas in [7] it was proposed to change the outlet temperature set point according to the value of the solar radiation. Therefore, in [15] the controlled variable is the superheating temperature, while in [7] it is the oil outlet temperature. In this paper the issue of controlling optimally a field with partial radiation is handled, and to do so an entire field model is used in order to take into account not only the total incident radiation, that is the case of [7] and [15], but as well its distribution among each of the loops that constitute the solar field. With this model it is possible to simulate each loop of the field, instead of simulating only one of them and supposing that the behavior of the entire field is the same.

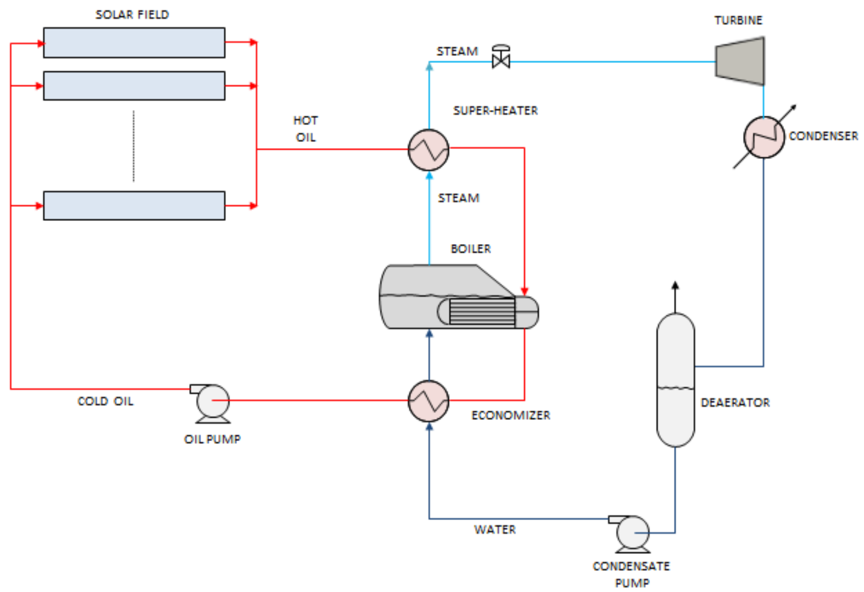

Figure 6.2: Diagram of the solar field connected with the power cycle

The use of a solar field model that individually takes into account all its loops was proposed in [1], but it was used to test a control strategy based on maximizing the outlet oil temperature of the field, which as said before it is not the optimal way to produce the maximum electrical power. However, in this paper this type of field model is used to compare two control strategies whose main objective is to maximize the electrical power, especially during days with partial covering. Both strategies consist of MPC controller, that uses predictions of the future clouds together with the collector field and power cycle models, although they differ in their number of manipulated variables. While one of the strategies proposed manipulates the total oil flow, which is then equally distributed among the loops, the other manipulates individually the oil flow circulating through each loop. With both strategies, an improvement of the electrical power generated is achieved, compared to the strategy of keeping constant the outlet oil temperature; however, it will be seen that the strategy that manipulates individually the flow of each loop does not produce a remarkable improvement compared to the one that manipulates the total flow.

The paper is organized as follows: Section 2 describes the models of the solar field, passing clouds and power cycle used for simulation purposes. Section 3 describes both control strategies tested: the global strategy, that consists of an MPC controller with only one manipulated variable (total oil flow) and the distributed strategy, that consists of an MPC controller with 24 manipulated variables (oil flow through each loop). Section 4 shows the results obtained by simulations made in MATLAB. Finally, the paper draws to a close with some concluding remarks.

6.2 SYSTEM MODELING

The model of each of the parts that have been used to simulate the operation of a solar field during days with partial covering is presented hereafter. These parts are: the solar collector field, the passage of the clouds, and the power cycle.

6.2.1 Solar Collector Field Model

The model of the solar collector field is the same used in [18] and in [20], being at the same time a slight modification of the model proposed by [3]-[6]-[8] for the ACUREX field (Fig. 6.1). Basically, this model can be used to simulate parabolic trough solar fields by selecting parameters like the number of active (the parts where the solar radiation reaches the tube) and passive (joints and other parts not reached by concentrated solar radiation) zones, the length of each zone, or the collector aperture. The solar field simulated in this paper is modeled using solar radiation data that correspond to the site of the Escuela Técnica Superior de Ingeniería de Sevilla. It is composed of 24 loops and has dimensions of 144x240 m. Each loop is modeled by the following system of partial differential equations that describe the energy balance:

Active zones

$$\rho_m C_m A_m \frac{\partial T_m}{\partial t} = I n_0 G - H_l G(T_m - T_a) - dH_t(T_m - T_f), \tag{6.1}$$

Fluid element

$$\rho_f C_f A_f \frac{\partial T_f}{\partial t} + \rho_f C_f \dot{q} \frac{\partial T_f}{\partial x} = dH_t(T_m - T_f), \tag{6.2}$$

Passive zones

$$\rho_m C_m A_m \frac{\partial T_m}{\partial t} = -GH_p(T_m - T_a) - dH_t(T_m - T_f), \qquad (6.3)$$

where the sub-index m refers to metal and f refers to the fluid. The model parameters and their units are shown in table 6.1.

Table 6.1: Solar field model parameters and variables description

Symbol	Description	Units
t	Time	s
x	Space measured along the tube	m
ρ	Density	Kg/m^3
C	Specific heat capacity	J/(K kg)
A	Cross sectional area	m^2
T	Temperature	°C
$\dot{q}$	Oil flow rate	m^3/s
I	Solar radiation	W/m^2
n_0	Optical efficiency	Unit-less
G	Collector aperture	m
T_a	Ambient Temperature	°C
H_l	Global coefficient of thermal losses for active zones	W/(m^2 °C)
H_t	Coefficient of heat transmission metal-fluid	W/(m^2 °C)
H_p	Global coefficient of thermal losses for passive zones	W/(m^2 °C)
d	Pipe diameter	m

The density ρ and specific heat C depend on the fluid temperature [3]. The coefficient of heat transmission H_t depends on temperature and oil flow [3]. The incident solar radiation I, that includes the cosine and incident angle modifier effects, depends on hourly angle, solar hour, declination, Julianne day, and local latitude [3]-[6]-[8]. The pipe has a length of 480 m (432 m of active zones and 48 m of passive zones) and a cross sectional area of $5.3 * 10^{-4}$ m^2. The collector aperture is 1.82 m and the optical efficiency is 0.675. The coefficient of thermal losses for active zones, H_l, and for passive zones, H_p, has a value of 0.49 and 0.24 respectively. These values are assumed to be constant. Although they vary with temperatures and since the ambient temperature has very little influence on solar field efficiency [16], this assumption is acceptable for the purposes of the current work. In order to solve this system of partial differential equations, a two stage finite difference equation has been programmed, considering each segment of 1 m for the passive zones and of 3 m for the active zones [3] and solving (6.1)-(6.2)-(6.3).

This solar field model is connected to a power cycle model (Fig.6.2) as commented in section 1 and further described below. Both models have to be simulated simultaneously because some of their variables are shared. Specifically, to simulate the field, the value of the inlet temperature is needed and it can only be obtained after solving the equations of the cycle model. At the same time, to simulate the power cycle, the outlet temperature and the oil flow are needed. Therefore, the simulation of both models is an iterative process.

6.2.2 Modeling of the Passing Clouds

The modeling of the passing clouds is necessary to know how the solar radiation is distributed throughout the field. This can be achieved by creating a matrix that represents the whole field extension. Each element of the matrix is assigned the value of the incident solar radiation on that section at each time. The solar field has dimensions of 144x240 m so, if the field is divided in elements of 3x3 m, a 48x80 matrix is needed. The matrix is then put over the field in such a way that each element contains a fraction of an active or passive element. Figure 6.3 shows the fraction of the whole matrix that covers one loop of a generic field.

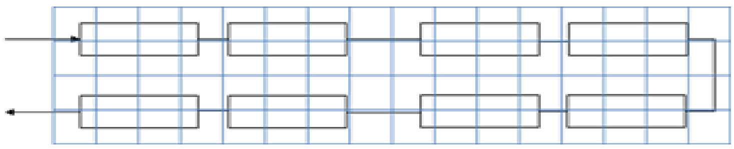

Figure 6.3: Example of a fraction of the matrix over one loop of the field

The value of the radiation in each element of the matrix depends on the following parameters:

- The Direct Normal Irradiation (DNI) on the field.
- The direction of the route followed by the passing cloud (the angle formed by this direction and the direction followed by the thermal fluid, being 0 degrees the direction which is the same one followed by the thermal fluid and 90 degrees the perpendicular).
- The velocity of the passing cloud (determined by the number of elements of the matrix supposed to be traveled by the cloud every 39 seconds, which is the sample time of the field).

- The size of the cloud (a rectangular form is supposed, defined by the number of rows and columns that it covers).
- The attenuation factor, that is the value that multiplies the radiation in the zones where the cloud is present. This value varies between 0 and 1 depending on the radiation that the cloud allows to reach the field, being 0 the case in which no radiation reaches the field, and 1 the case in which all the radiation reaches it.

Once these values are set, the program calculates for each collector the mean value of radiation of every element of the matrix related with it. This mean value is assigned to the variable I of (6.1).

The velocity values used in the model are quite small. The reason of these values is that the solar field used for simulation is also small; therefore if real cloud velocities are simulated they scarcely produce any effect on the field due to the minimum time of permanence over the field. For that reason, in order to simulate a time of permanence similar to that of the commercial plants, a lower velocity is assumed.

6.2.3 Power Cycle Model

The Rankine power cycle simulated in this paper consists of an economizer, a boiler and a super-heater (each one denoted by the subscript E, B and S respectively) followed by a steam turbine.

Following the path traveled by the oil flow (Fig. 6.2), it first enters into the super-heater where the steam flow is overheated to a certain temperature. This super-heater was modeled by the equations

$$\begin{aligned} m_o C_{Po} T_{io} - Q_S &= m_o C_{Po} T_{oo}, \\ m_s C_{Ps} T_{is} + Q_S &= m_s C_{Ps} T_{os}, \\ Q_S &= U_S A_S LMTD_S, \end{aligned} \tag{6.4}$$

that form a system of three equations and three unknown values. The unknown values are the outlet oil and outlet steam temperatures, T_{oo} and T_{os} respectively, and the heat exchanged in the super-heater Q_S. The heat exchangers (E, B and S) have been designed by following the typical rule that the temperature difference at each outlet of each heat exchanger for the nominal operating point (900W/m^2 of solar radiation and 393°C of oil outlet temperature) was higher than 10°C. This allows the values of the product of the thermal transmittance U and the exchange area A of each exchanger to be set (table 6.2). Then, the supposition that these values are constant was made, assuming the associated errors due to the slight variation of U. The specific heat of both, the oil C_{Po}, and the steam C_{Ps} depend on the fluid temperature, the first one being calculated by the polynomial function in [3] and the second one using the steam property tables. The mass flow m_o, and the inlet temperature T_{io} of the oil were given by the solar field model and the mass flow m_s, and the inlet temperature T_{is} of the steam as given by the boiler model that will be shown below. Finally, the logarithmic mean temperature difference $LMTD$ needed in one of the equations is calculated using the equation

$$LMTD = \frac{(T_{io} - T_{os}) - (T_{oo} - T_{is})}{\ln\left(\frac{(T_{io}-T_{os})}{(T_{oo}-T_{is})}\right)}. \tag{6.5}$$

Table 6.2: Values of UA

Parameter	Value (kJ/s °C)
$U_S A_S$	20.15
$U_B A_B$	96.95
$U_E A_E$	25

After the super-heater, the oil flow is used to boil the water flow to produce saturated steam in the boiler. This process is carried out at a floating pressure to maximize the amount of heat exchanged. The equations used to model the boiler are

$$\begin{aligned} m_o C_{Po} T_{io} - Q_B &= m_o C_{Po} T_{oo}, \\ m_w C_{Pw} T_{iw} + Q_B &= m_s H_v + m_w C_{Pw} T_{ow}, \\ Q_B &= U_B A_B LMTD_B. \end{aligned} \tag{6.6}$$

Again, these equations form a system of three equations and three unknown values, which are the outlet oil and outlet steam temperatures, T_{oo} and T_{os} respectively, and the heat exchanged in the boiler, Q_B. Due to the fact that a steady state model is considered, the water flow m_w is equal to the steam flow m_s. The heat of vaporization H_v can be found in the steam tables or computed by polynomial functions that depend on the pressure or temperature. The remaining variables can be obtained as in the previous paragraph.

Finally, the oil flow is introduced into an economizer where it is used to preheat the water flow, and is then recycled to the field. The economizer is modeled by the equations

$$\begin{aligned} m_o C_{Po} T_{io} - Q_E &= m_o C_{Po} T_{io} T_{oo}, \\ m_w C_{Pw} T_{iw} + Q_E &= m_w C_{Pw} T_{ow}, \\ Q_E &= U_E A_E LMTD_E. \end{aligned} \tag{6.7}$$

In this case, as in the previous ones, we have a system of three equations and three unknowns, that are the outlet oil and outlet steam temperatures, T_{oo} and T_{os} respectively, and the heat exchanged in the economizer Q_E. The other variables are calculated as explained in the super-heater.

The steam generated in the super-heater flows into a high pressure turbine. In order to model this turbine the Willan's Line Method described in [24] is used. First, the turbine outlet pressure is set at a value of 5.63 kPa, which is a typical value for condensation turbines because it allows the use of water at ambient temperature to condensate the steam. Then, to calculate the inlet pressure, the equation

$$P_i = k m_s \tag{6.8}$$

is used, which is a modification of the Stodola equation [25] when the inlet pressure is far higher than the outlet one, as it is the case. With these pressure values it is possible to compute the saturation temperatures of the inlet and the outlet steam flow, so that the difference of saturation temperature ΔT_s could be known and subsequently used in

$$\begin{aligned} a &= 0.662 \Delta T_s \\ b &= 1.191 + 0.000759 \Delta T_s \end{aligned} \tag{6.9}$$

to calculate parameters a and b if the generated power by the turbine is lower or equal than 2000 kW, and in

$$\begin{aligned} a &= -463 + 3.53 \Delta T_s \\ b &= 1.220 + 0.000148 \Delta T_s \end{aligned} \tag{6.10}$$

if it is higher than 2000 kW.

After that, it is necessary to calculate the isentropic difference of enthalpy ΔH_i and to set the parameter L which is the interception rate that depends on the turbine characteristics, its typical value being between 0.05 and 2.

With these two parameters and with a and b we can calculate n and W_{int} using

$$\begin{aligned} n &= \frac{(L+1)}{b}(\Delta H_i - a/m_s), \\ W_{int} &= \frac{L}{b}(\Delta H_i m_s - a), \end{aligned} \tag{6.11}$$

and with them, using

$$W = nm_s - W_{int}, \tag{6.12}$$

we can calculate the electrical power generated by the turbine.

The model was simulated using the software Engineering Equation Solver© and then with these simulation results two polynomial functions of the oil outlet temperature and mass flow

$$W = 8230 - 49.96m_{oil} - 2.7m_{oil}^2 - 47.15T_{out} + 0.068T_{out}^2 + 0.54m_{oil}T_{out}, \tag{6.13}$$

and

$$T_{in} = 340 + 1.78m_{oil} - 0.155m_{oil}^2 - T_{out} + 0.0011T_{out}^2 + 0.022m_{oil}T_{out}, \tag{6.14}$$

were obtained in order to calculate the electrical power generated and the oil temperature returning to the field respectively. This simplification was necessary to reduce the simulation time, while keeping the error around 1%. In addition, the dynamic of the cycle was assumed to be like a first order model with a time constant of 100 seconds, that is the dynamic of the slowest part of the cycle, the boiler. The power cycle was modeled using the software Aspen Hysys© and the time constant was obtained by simulation.

The net electrical power produced by the field is the result of subtracting the power consumed by the pump to the power generated by the turbine. Therefore, to calculate the consumption of the pump the Darcy equation is used to estimate the pressure loss hpl

$$hpl_i = 9806.65\frac{8fl\dot{q_i}^2}{g\pi^2 d^5}. \tag{6.15}$$

The Reynolds number Re and the Barr's friction coefficient f needed are computed by

$$Re_i = \frac{\rho_f \dot{q}_i d}{A_f \mu} \tag{6.16}$$

and

$$f_i = 0.25 \frac{1}{(log10(\frac{\epsilon_r}{3.7d} + \frac{5.74}{Re_i^{0.9}}))^2} \tag{6.17}$$

respectively.

The power consumption W_{pump} depends on the pump efficiency η_{pump}, oil flow q and the pressure loss hpl from

$$W_{pump} = \sum_{i=1}^{i=24} \frac{\dot{q}_i hpl_i}{\eta_{pump}}. \tag{6.18}$$

Finally, the net electrical power is calculated by

$$W_{net} = W - \frac{W_{pump}}{1000}(kW). \tag{6.19}$$

A summary of the model parameters and their units is shown in Table 6.3.

Table 6.3: Power cycle model parameters and variables description

Symbol	Description	Units
Q	Exchanged heat	kW
m	Mass flow	kg/s
C	Specific heat capacity	kJ/(K kg)
A	Exchange area	m^2
T	Temperature	°C
U	Thermal transmittance	kW/(m^2 °C)
$LMTD$	Logarithmic mean temperature difference	°C
H	Enthalpy	kJ/kg
P	Pressure	kPa
a	Correlating parameter for steam turbines	kW
b	Correlating parameter for steam turbines	Unit-less
L	Interception rate	Unit-less
n	Slope of the Willans' Line	kW/kg
W_{int}	Willans' Line intercept	kW
ρ_f	Fluid density	Kg/m^3
$\dot{q}$	Oil flow	m^3/s
A_f	Cross sectional area	m^2
μ	Dynamic viscosity	Kg/(m s)
d	Pipe diameter	m
ϵ_r	Relative rugosity	m
g	Gravity	m/s^2
l	Loop length	m
pd	Pressure drop	Pa

6.3 CONTROL STRATEGIES

In this section two control strategies are presented. Both strategies consist of MPC controller with the same prediction and control horizons, prediction model and constraints, but with different manipulated variables. The first one, called by the authors as the global strategy (GS), manipulates the total oil flow circulating through the field, assuming that this flow is equally divided among the 24 loops of the field. The other one, named distributed strategy (DS), manipulates separately the oil flow circulating through each loop, which means that it has 24 manipulated variables. In both strategies one main pump is installed plus valves that are manual in the GS case and automatic in the DS case. The loops are treated as non-coupled.

6.3.1 Global Strategy

The Global control strategy is based on using MPC controller, that uses models of the field, the power cycle, and predictions of the passing clouds through the field, so that the controller calculates the optimum value of oil outlet flow that maximizes the electrical power generated, taking into account temperature and oil flow constraints. The solar collector field model used by the MPC is a simplification of the one used to simulated the real field (6.1)-(6.2), which assumes that the pipe is only divided in 6 parts of 80 meters instead of the divisions of 1 meter for passive zones and 3 meters for the active zones. The prediction of the passing clouds has been made assuming that the exact position of the cloud is known for each sampling interval of the prediction horizon, although the value of the incident solar radiation is supposed to be constant for each sampling interval, which adds some degree of error between the predicted value and the real one. The control structure can be seen in figure 6.4.

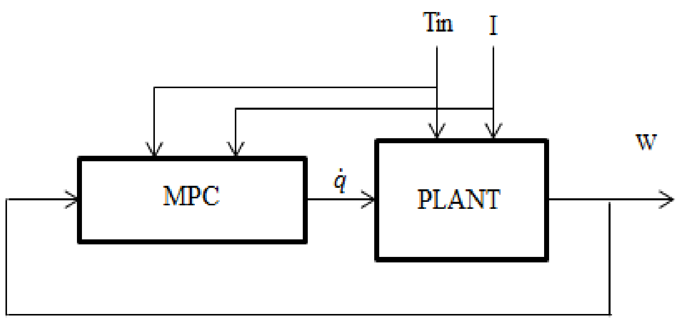

Figure 6.4: Global strategy controller

The electrical power generated is considered along an extended period of time, from time $(k+1)h$ up to some horizon $(k+H)h$, where k denotes present discrete time, H is the prediction horizon, and h is the sampling interval, which in this case has a value of 39 seconds. Therefore, the aim is to select the flow that optimizes the multistep cost function

$$J(\dot{q}_k^{k+H-1}) = \sum_{i=1}^{H} W_{net}(\dot{q}((k+i-1)h)). \tag{6.20}$$

The maximization of J is performed with a receding horizon strategy, using a prediction horizon of H=12 and a control horizon of 3. The value of the prediction horizon was chosen after making some simulations for different values of it, and selecting the one that allowed to produce the highest amount of electrical power during an operating day. The results of these simulations can be seen in figure 6.5. A control horizon of 3 was selected due to the fact that with a higher one the improvement achieved in the amount of electrical power was less than 0.1% and also increased the calculation time of the optimizer.

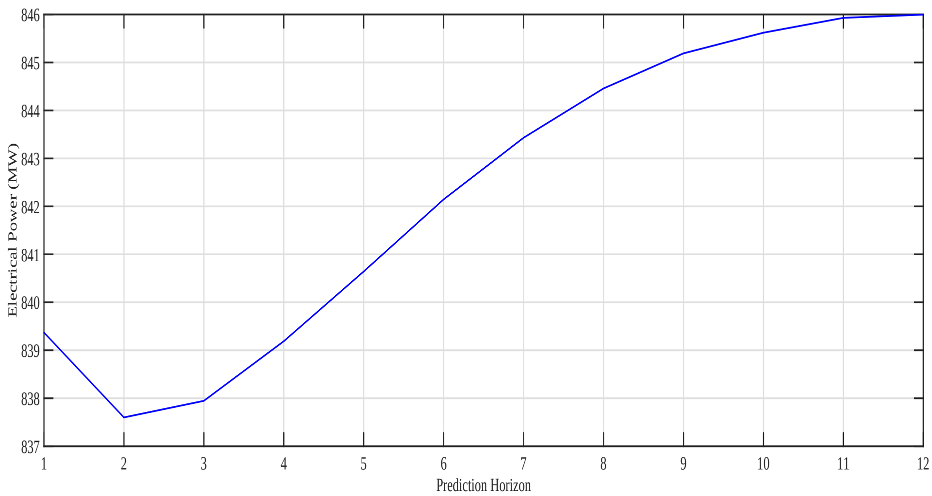

Figure 6.5: Electrical power generated for different values of the prediction horizon

The dynamic optimization procedure may be expressed as the following algorithm:

- All the variables needed by the field and cycle model are measured.
- The simplified solar collector field model is used to calculate the outlet oil temperature of the field. The oil flow ($\dot{q}$) is the independent variable used by the optimizer.
- With the values of the oil outlet temperature and mass oil flow, equations (6.13) and (6.14) are used to calculate the electrical power generated by the turbine (W) and the inlet oil temperature (T_{in}).
- Finally, with equations (6.16), (6.17), (6.15), (6.18) and (6.19), the net electrical power is calculated (W_{net}).

Therefore, the MPC has to maximize the value of net electrical power subject to restrictions in oil temperature ($T \leq 400$°C) and oil flow (0.133 $l/s \leq \dot{q} \leq 1.58$ l/s) for each loop. The optimization is carried out for each integration step by the function $fmincon$ in MATLAB. The optimum value of oil flow is then sent as the new set point of the flow controller, which manipulates the variable frequency drive. In this simulation, the dynamics of the flow controller plus the dynamics of the pump and the hydraulic circuit are assumed to be like a second order system.

6.3.2 Distributed Strategy

The Distributed control strategy is mainly the same as the previous one (GS), but with the difference that instead of calculating the total oil flow of the field, the MPC calculates the value of the oil flow that should circulate through each loop in order to maximize the electrical power generated, taking into account temperature and oil flow constraints. The control scheme can be seen in figure 6.6.

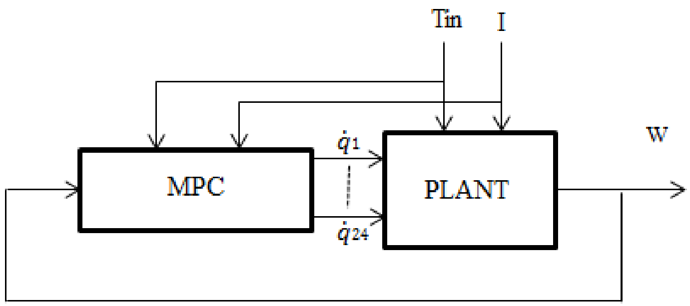

Figure 6.6: Distributed strategy controller

The optimization is also carried on the same way that in the global strategy, but the output of the MPC consists now of 24 variables, each one corresponding to the value of the oil flow of each loop. The increase in the number of variables leads to an increase in the calculation time on each integration step of the optimizer. However, the calculation of each integration step of the whole program (including the MPC, solar field, passing clouds and power cycle) requires around 20 seconds to simulate a period of 39 seconds, and may therefore be implemented in a real plant.

6.4 SIMULATION RESULTS

This section of the article shows the results obtained by simulations made with the models described in the previous sections. The aim of these simulations is to compare the performance of the global and the distributed strategies during situations of partial coverage of the solar field by passing clouds. The passing clouds have been simulated with the model described in section 2 with the following parameters: a matrix of 16x16, a velocity of 2 matrix elements per integration step, a direction of 45° and an attenuation factor of 0. However, for each simulation the time of passage has been modified. This time of passage has been defined as the number of integration steps where there is no cloud over the field after the last one had abandoned it; that criteria means that during all the simulation there are passing clouds entering and leaving the field, separated by this time.

The first of these simulations has been carried out with a time of passage of 40 steps, resulting on the solar radiation curve shown in figure 6.7. With this radiation curve, both control strategies were assessed along with the one used to keep constant the outlet temperature of the field, in order to see if the distributed strategy achieved an improvement in the electrical power generated, but as can be seen in figures 6.8, 6.9, and 6.10 both strategies have a similar behavior, the improvement achieved by the distributed one being negligible. The oscillatory behavior of the strategy used to keep constant the outlet temperature of the field is due to the use of a static feedforward without dynamic compensation. In addition, it can be seen in figure 6.10 that the oil flow is nearly constant, which is a good thing for the proper operation of the pump and also implies that the assumption made in section 2 about using a constant value of U is correct.

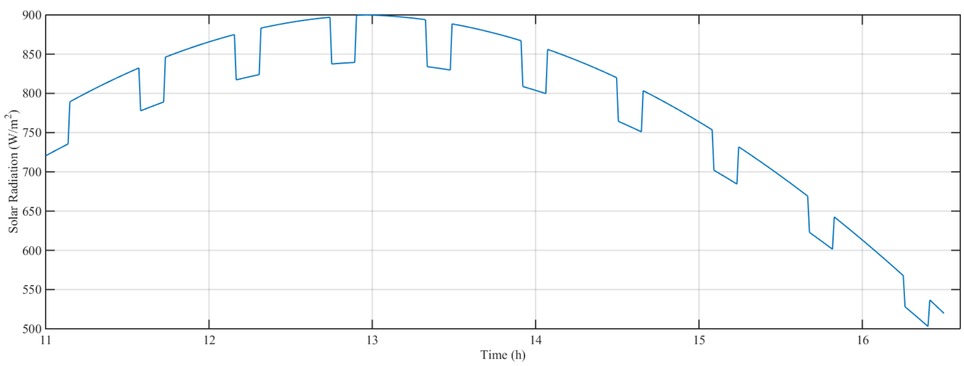

Figure 6.7: Average incident solar radiation

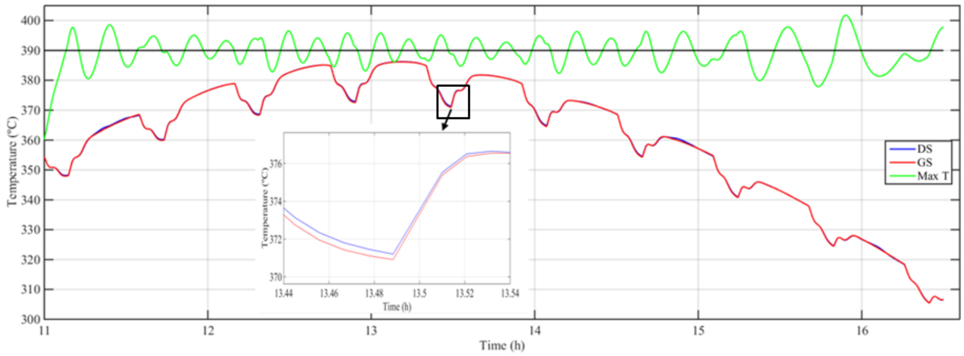

Figure 6.8: Oil outlet temperature of the field obtained with the global and distributed strategies

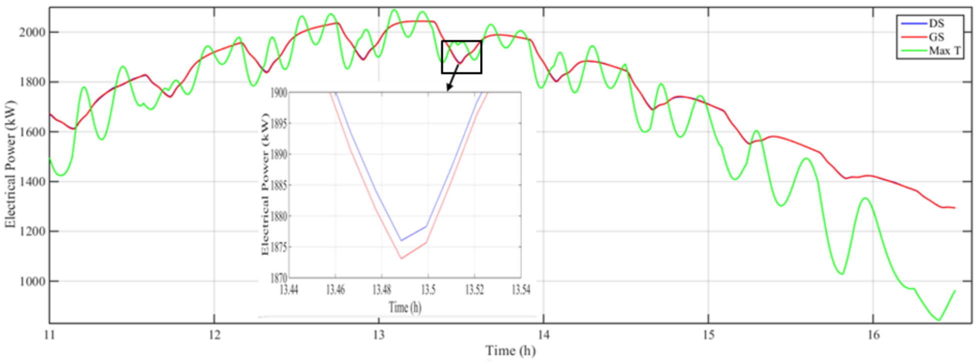

Figure 6.9: Electrical power generated by the global and distributed strategies

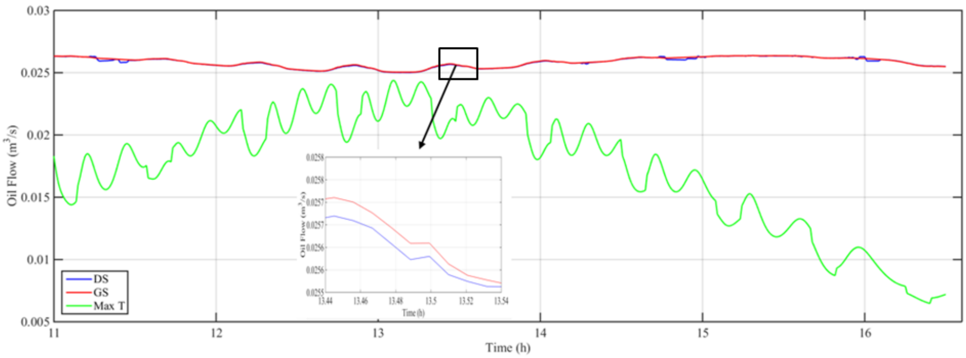

Figure 6.10: Oil flow with the global and distributed strategies

The remaining simulations consist of testing these strategies for different times of passage, starting from a time of 15 until 100 every five. In addition, a clear day was simulated to have it as baseline. Figure 6.11 shows the results of electrical power generated by each strategy for each time of passage; it also shows the power generated by a control strategy that tries to keep constant the outlet oil temperature of the field instead of maximizing the electrical power. This last strategy is similar to the one proposed in [1], which as can be seen in figure 6.11 results in a loss of power. Figure 6.12 shows the percentage of improvement achieved with the strategies proposed in this paper compared with the one that keeps constant the outlet temperature for each time of passage of the clouds. It is clear that, the lower the time of passage of the clouds, the higher the improvement achieved. However, the main improvement is not due to the presence of clouds (this improvement is about 1-1.5% depending on the number of passing clouds), but to the adaptation of the outlet oil temperature to the curve of solar radiation, as can be seen in figure 6.12, taking the value of the improvement achieved when there are no clouds as reference (about 4%). The reason of that, it is due to the fact that the maximum electrical power depends on the oil flow and outlet temperature and therefore, during a clear day both strategies behave in the same way since they calculate the same value of oil flow and so, the same value of outlet temperature. However, when a cloud is present, the loop temperature constraint makes the DS strategy to behave better due to its capacity of manipulating the flow of each loop instead of the total one. This improvement depends on the loops covered by the cloud and the time of passage. The greater the number of loops covered, the greater the improvement achieved, but there is a maximum between the case of a clear day and the case in which all the field is covered by clouds; cases in which no improvement can be achieved. This fact implies that the maximum is so tightly bounded, that the improvement will be always negligible.

Another advantage of using the GS or the DS strategies is that with them the problem of having temperature peaks is avoided. This problem takes place while using the control strategy that keeps constant the oil outlet temperature and a cloud passes through the field. When this situation happens, the controller lowers the oil flow in order to maintain the same value of temperature, but in doing so, the loops that are not covered by the cloud may have their temperature increased above the security limit of 400°C, causing mirrors to get out of focus. That situation would lead to a further loss in power not considered here. A more detailed explanation of this problem can be found in [19].

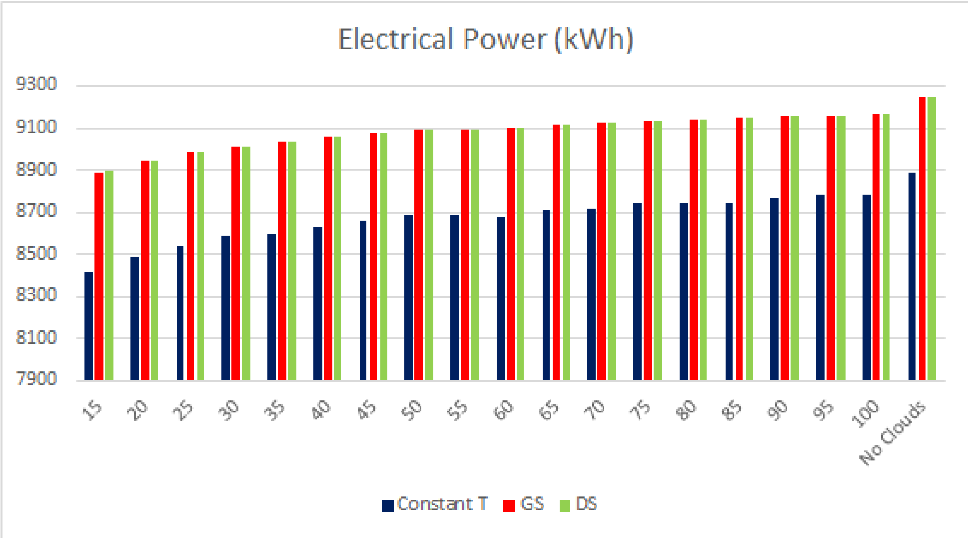

Figure 6.11: Electrical power generated for different pass frequencies of the clouds, by the global and distributed strategies and a control strategy which tries to keep constant the oil outlet temperature at 390°C

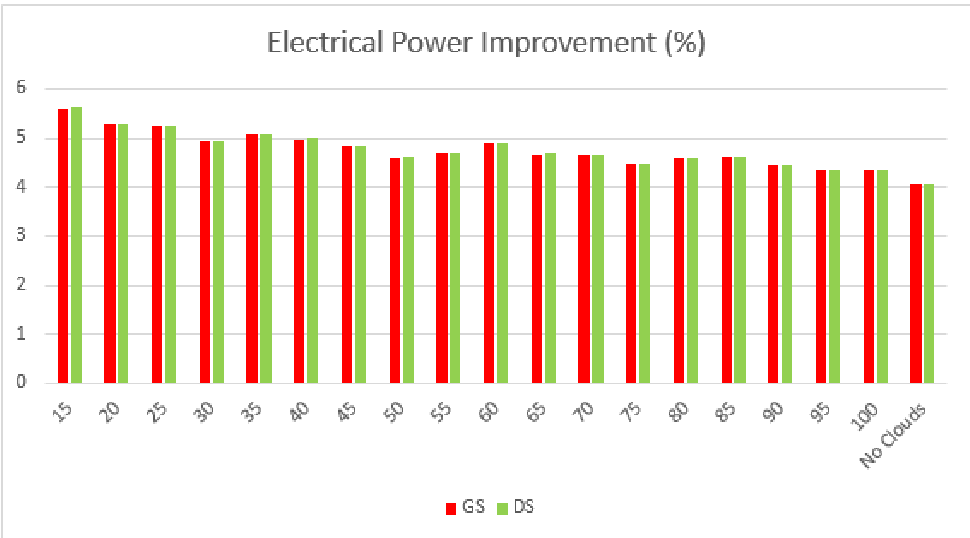

Figure 6.12: Percentage of improvement achieved by operating at optimum temperature rather than at a constant temperature of 390°C

6.5 CONCLUSIONS

The main conclusion of this paper is that both MPC strategies proposed achieve a higher production of electrical power compared with a strategy with a fixed set point of temperature (around 390°C).The improvement achieved is between 4% for clear days and 5.7% for cloudy days. Although this improvement is mainly due to the adaptation of the outlet oil temperature to the curve of solar radiation, if the number of clouds passing through the field is high, the improvement could be increased in 1.7% compared to the case with no clouds. Therefore it can be deduced that the improvement achievable by applying this strategies are dependent of the presence of the clouds, but still improve the electrical power obtained with a maximum temperature strategy, even when there are no clouds over the field.
Another conclusion is that the use of a control strategy that manipulates individually the oil flow circulating through each loop in order to maximize the electrical power generated by the plant does not produce any significant improvement compared with the one which manipulates the total oil flow that is divided equally among the loops.
Regarding the solar commercial plants; the results obtained in this paper could be applied to them by scaling the prediction model of their different parts (solar collector field, power cycle, and cloud matrix) used by the MPC, because these strategies were assessed in conditions normally used in commercial plants despite the differences in size.

Bibliography

[1] Abutayeh, M., Alazzam, A. and El-Khasawneh, B. (2014). *Balancing heat transfer fluid flow in solar fields.* Solar Energy, 105, 381-389.

[2] Barão, M., Lemos, J. and Silva, R. (2002). *Reduced complexity adaptive nonlinear control of a distributed collector solar field.* Journal of Process Control, 12-1, 131-141.

[3] Camacho, E. F., Berenguel, M. and Rubio, F. (1997). *Advanced control of solar plants.* Springer-Verlag, London.

[4] Camacho, E. F., Rubio, F. R., Berenguel, M. and Valenzuela, L. (2007). *A survey on control schemes for distributed solar collector fields. Part I: Modeling and basic control approaches.* Solar Energy, 81-10, 1240-1251.

[5] Camacho, E. F., Rubio, F. R., Berenguel, M. and Valenzuela, L. (2007). *A survey on control schemes for distributed solar collector fields. Part II: Advanced control approaches.* Solar Energy, 81-10, 1252-1272.

[6] Camacho, E. F., Berenguel, M., Rubio, F. R. and Martínez, D. (2012). *Control of solar energy systems.* Springer-Verlag, London.

[7] Camacho, E. F. and Gallego, A. (2013). *Optimal operation in solar trough plants: A case study.* Solar Energy, 95, 106-117.

[8] Carmona, R., (1985). *Análisis, modelado y control de un campo de colectores solares distribuidos con sistema de seguimiento en eje.* Ph.D. Thesis.

[9] Cirre, C., Berenguel, M., Valenzuela, L. and Camacho, E. F. (2007). *Feedback linearization control for a distributed solar collector field.* Control Engineering Practice, 15-12, 1533-1544.

[10] Cirre, C., Berenguel, M., Valenzuela, L. and Klempous, R. (2009). *Reference governor optimization and control of a distributed solar collector field.* European Journal of Operational Research, 193, 709-717.

[11] Colmenar-Santos, A., Munuera-Perez, F., Tawfik, M. and Castro-Gil, M. (2014). *A simple method for studying the effect of scattering of the performance parameters of parabolic trough collectors on the control of a solar field.* Solar Energy, 99, 215-230.

[12] Gallego, A. and Camacho, E. F. (2012). *Estimation of effective solar irradiation using an unscented kalman filter in a parabolic-trough field.* Solar Energy, 86-12, 3512-3518.

[13] García, S. (2012). *Guía técnica de la energía solar termoeléctrica* Fenercom, Capítulo 1.

[14] Lima, D., Normey-Rico, J. and Santos, T. (2016). *Temperature control in a solar collector field using filtered dynamic matrix control.* ISA Transactions, 62, 39-49.

[15] Lippke, F. (1995). *Simulation of the part-load behavior of a 30 MWe SEGS plant.* Report No. SAND95-1293, SNL, Albuquerque, NM, USA.

[16] Manzolini, G., Giostri, A., Saccilotto, C., Silva, P. and Macchi, E. (2012). *A numerical model for off-design performance prediction of parabolic trough based solar power plants.* Journal of Solar Energy Engineering, Vol.134.

[17] Montes, M., Abánades, A., Martínez-Val, J. and Valdés, M. (2009). *Solar multiple optimization for a solar-only thermal power plant, using oil as heat transfer fluid in the parabolic trough collectors.* Solar Energy, 83-12, 2165-2176.

[18] Navas, S. J., Rubio, F. R., Ollero, P. and Ortega, M. G. (2016). *Modeling and simulation of parabolic trough solar fields with partial radiation.* XV European Control Conference, 31-36.

[19] Navas, S. J., Rubio, F. R. and Ollero, P. (2017). *Optimum control of parabolic trough solar fields with partial radiation.* IFAC-PapersOnLine, Vol.50-1, 109-114.

[20] Navas, S. J., Ollero, P. and Rubio, F. R. (2017). *Optimum operating temperature of parabolic trough solar fields.* Solar Energy, 158, 295-302.

[21] Price, H., Lupfert, E., Kearney, D., Zarza, E., Cohen, G., Gee, R. and Mahoney, R. (2002). *Advances in parabolic trough solar power technology.* Solar Energy, 124-2, 109-125.

[22] Rubio, F. R., Camacho, E. F. and Berenguel, M. (2014). *Control of solar collector fields.* Revista Iberoamericana de Automática e Informática Industrial (RIAI), 3-4, 26-45.

[23] Shinskey, F. (1978). *Energy conservation through control.* Academic Press.

[24] Smith, R. (2005). *Chemical process design and integration.* Wiley.

[25] Stodola, A. (1945). *Steam and gas turbines.* Vol. 1, Peter Smith, New York.

Chapter 7

Paper 3

Control of a distributed solar collector field with thermal energy storage and partial radiation
Sergio J. Navas, Francisco R. Rubio, Pedro Ollero, and João M. Lemos. Paper under review submitted to the journal "Journal of Process Control".

This paper describes and assesses a new optimal strategy to control distributed solar collector fields with thermal storage systems, especially during days in which the field is under partial radiation due to the passage of clouds. The main objective of this control strategy is to maximize the thermal energy stored while keeping the net electrical power produced close to its reference value, during situations in which different parts of the solar field receive different degrees of solar radiation. Simulations were carried out using three connected models, one for the solar field (taking into account all of its loops individually) that includes the passage of clouds, another one for the thermal storage system, and finally one for the power cycle. The results obtained with this new control strategy have been compared to the usual control strategy based on keeping the outlet oil temperature constant at a value around 390° C, with the result of achieving an average improvement in hours of electrical power production between 4% and 12%.

7.1 INTRODUCTION

For some time now, there has been a growing interest in the use of solar energy, and specifically of solar thermal power plants. The Concentrated Solar Thermal Power Plants (CSTPP) are systems used to get electric power from solar energy by pre-transforming it into thermal energy that have the major advantage of allowing energy storage. This paper focuses on parabolic trough solar fields, that consist of a collector field, a power cycle, a thermal storage system, and auxiliary elements such as pumps, pipes, and valves (Fig. 7.1). The solar collector field collects solar radiation and focuses it onto a tube in which a heat transfer fluid, such as thermal oil, circulates. The oil is heated up and then used by the power cycle to produce high pressure steam in a boiler, and electricity by expanding it in a turbo-generator. Alternatively, part of the oil flow can be directed to the thermal storage system when there is an excess of energy collected by the field. The models of the solar plant used in this paper are based on a pilot plant [4] with a nominal power production of 1200 kW.

The main goal of a parabolic trough solar field with a thermal storage system is to collect solar energy in order to produce the contracted electrical power while storing the maximum amount of thermal energy to continue producing the contracted electrical power when the level of incident solar radiation is not enough for the solar field to produce it. Therefore, some studies like [3] aims to optimize the designing of these plants. During the operation, most of the solar thermal power plants try to achieve this main goal by keeping the outlet oil temperature of the field around the maximum allowable value (400°C) imposed to prevent oil degradation; although some studies like [8] and [11] show that this way to operate the field is not optimal and leads to a loss in the thermal energy collected and so, in the electrical power generated. However, these studies were performed with plants without thermal storage systems, whereas other studies, like [2] show the importance of having a thermal storage system, especially during strongly cloudy days. For that reason, in this paper the issue of optimally controlling a field with a thermal storage system is handled. In addition, in order to assess the optimal control strategy proposed in this paper during days in which different parts of the solar field receive different degrees of solar radiation, such as strongly cloudy days, an entire field model is used in order to take into account not only the total incident radiation but as well its distribution among each of the loops that constitute the solar field. With this model it is possible to simulate each loop of the field, instead of simulating only one of them and supposing that the behavior of the entire field is the same.

The use of a solar field model that individually takes into account all its loops was proposed in [1], but it was used to test a control strategy based on maximizing the outlet oil temperature of the field, which as said before is not the optimal way to operate these fields. In this paper this type of field model is used to assess a new optimal control strategy whose main objective is to maximize the thermal energy stored while producing the contracted value of electrical power. This new control strategy consists of a MPC controller, that uses predictions of the future clouds together with the collector field and power cycle models to calculate the total oil flow, which is then equally distributed among the loops, and the oil flow sent to the storage system. This optimal strategy is compared to a strategy similar to the one used by commercial plants, which is based on keeping constant the outlet oil temperature, in order to show the level of improvement that can be achieved with it.

The paper is organized as follows: Section 2 describes the models of the solar field, passing clouds, power cycle and thermal storage system used for simulation purposes. Section 3 describes both control strategies tested: the constant temperature strategy and the optimal control strategy. Section 4 shows the results obtained by simulations made in MATLAB. Finally, the paper draws to a close with some concluding remarks.

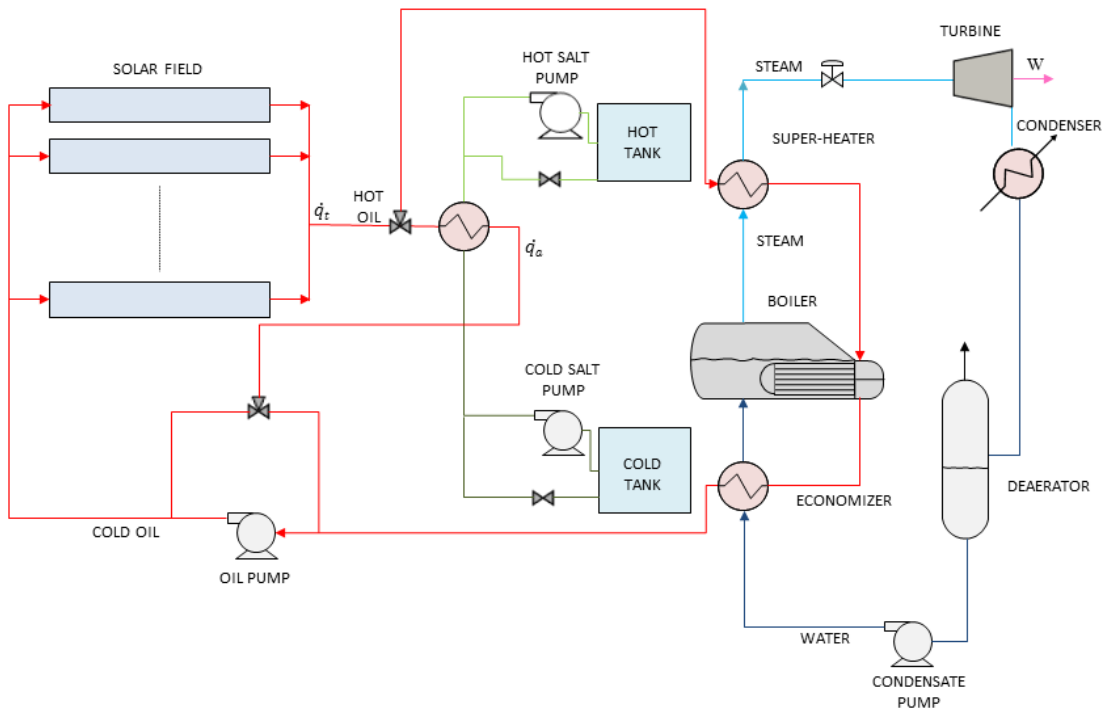

Figure 7.1: Scheme of the solar field, including energy storage in the hot tank, connected to the power cycle

7.2 SYSTEM MODELING

The model of each of the parts that have been used to simulate the operation of a solar field during days with partial covering is presented hereafter. These parts are: the solar collector field, the passage of the clouds, the power cycle, and the thermal storage system.

7.2.1 Solar Collector Field Model

The solar collector field is based in the model proposed by [4]-[5]-[7], which has been used in many previous studies [9]-[13]-[6]. Basically, this model can be used to simulate parabolic trough solar fields by selecting parameters like the number of active (the parts where the solar radiation reaches the tube) and passive (joints and other parts not reached by concentrated solar radiation) zones, the length of each zone, or the collector aperture. The solar field simulated in this paper is modeled using solar radiation data that correspond to the site of the Escuela Técnica Superior de Ingeniería de Sevilla. It is composed of 24 loops and has dimensions of 144x240 m. The complete and detailed model can be found in [11].

This solar field model is connected to a power cycle model and a storage system model (Fig.7.1) as mentioned in section 1 and further described below. All models have to be simulated simultaneously because some of their variables are shared. Specifically, to simulate the field, the value of the inlet oil temperature is needed and it can only be obtained after solving the equations of the cycle model and the storage system model. At the same time, to simulate the power cycle and the storage system, the outlet temperature and the oil flow are needed. Therefore, the simulation of both models is an iterative process.

7.2.2 Modeling of the Passing Clouds

The modeling of the passing clouds is necessary to know how the solar radiation is distributed throughout the field. This can be achieved by creating a matrix that covers the whole field extension. Each element of the matrix is assigned the value of the incident solar radiation on that section at each time. The solar field has dimensions of 144x240 m so, if the field is divided in elements of 3x3 m, a 48x80 matrix is needed. The matrix is then put over the field in such a way that each element contains a fraction of an active or passive element.

The value of the radiation in each element of the matrix depends on the following parameters [12]:

- The Direct Normal Irradiation (DNI) on the field.
- The direction of the route followed by the passing cloud.
- The velocity of the passing cloud.
- The size of the cloud.
- The attenuation factor.

The cloud velocity values used in the model are quite small. The reason of these values is that the solar field used for simulation is also small; therefore if real cloud velocities are simulated they scarcely produce any effect on the field due to the minimum time of permanence over the field. For that reason, in order to simulate a time of permanence similar to that of the commercial plants, a lower velocity is assumed.

7.2.3 Power Cycle Model

The Rankine power cycle simulated in this paper consists of an economizer, a boiler and a super-heater followed by a steam turbine. Following the path traveled by the oil flow (Fig. 7.1), it first enters into the super-heater where the steam flow is overheated to a certain temperature. After the super-heater, the oil flow is used to boil the water flow to produce saturated steam in the boiler. This process is carried out at a floating pressure to maximize the amount of heat exchanged. Finally, the oil flow is introduced into an economizer where it is used to preheat the water flow, and is then recycled to the field. The steam generated in the super-heater flows into a high pressure turbine. This turbine has been modeled using the Willan's Line Method described in [14].

The complete and detailed model of the power cycle was already presented in [11]. The are only minor differences in the values of the product of the exchange area A and the thermal transmittance U (see table 7.1) in order to set the nominal electrical power at 1200 kW.

Table 7.1: Values of UA

Parameter	Value (kJ/s °C)
$U_S A_S$	13.31
$U_B A_B$	91.86
$U_E A_E$	2.17

That new model was simulated using the software Engineering Equation Solver© and then with these simulation results two polynomial functions of the oil outlet temperature and mass flow were obtained in order to calculate the electrical power generated

$$W = 682.4 - 22.96m_{oil} - 1.23m_{oil}^2 - 6.92T_{out} + 0.016T_{out}^2 + 0.29m_{oil}T_{out} \quad (7.1)$$

and and the oil temperature returning to the field

$$T_{in} = 67.89 + 1.64m_{oil} - 0.11m_{oil}^2 + 0.37T_{out} - 0.00028T_{out}^2 + 0.016m_{oil}T_{out} \quad (7.2)$$

This simplification was necessary to reduce the simulation time, while keeping the error around 1%. In addition, the dynamic of the cycle was assumed to be like a first order model with a time constant of 100 seconds, that is the dynamic of the slowest part of the cycle, the boiler. The power cycle was modeled using the software Aspen Hysys© and the time constant was obtained by simulation.

The power consumed by the pump, that will be an important factor for the optimization of the plant, can be obtained following the method used in [11].

7.2.4 Storage System Model

The storage system shown in figure 7.1 consists of a heat exchanger and two tanks of molten salts, whose composition is 40% of $NaNO_3$ and 60% of KNO_3. The cold tank contains salt at 291°C that will be heated in the heat exchanger using the outlet oil of the solar field, whose thermal energy is intended to be stored. The heated salt flow is sent to the hot tank, where it is stored until it is needed to heat the oil of the solar plant in order to keep the electrical power production when there is not enough solar radiation.

Each tank is modeled by a mass balance

$$\rho_s \frac{\partial V}{\partial t} = \dot{m}_{in} - \dot{m}_{out}, \quad (7.3)$$

and an energy balance

$$\rho_s C_s V \frac{\partial T}{\partial t} = C_s \dot{m}_{in}(T_{in} - T) - C_s \dot{m}_{out}(T_{out} - T) - H_s(T - T_{amb}), \quad (7.4)$$

where V is the tank volume, $\dot{m}$ is the mass flow, T is the molten salt temperature in the tank, T_{amb} is the ambient temperature, H_s is the coefficient of thermal losses, ρ_s is the density and can be computed by

$$\rho_s = 2090 - 0.636T, \tag{7.5}$$

and C_s is the specific heat capacity defined by

$$C_s = 1443 - 0.172T. \tag{7.6}$$

The coefficient of thermal losses H_s has a value of 0.015 W/°C. This value has been calculated by assuming that the tank loses 1°C of temperature per day at maximum volume capacity, an ambient temperature of 25°C, and a salt temperature of 380°C .

The heat exchanger has been modeled by the equations

$$\begin{aligned} m_o C_{Po} T_{io} - Q_{St} &= m_o C_{Po} T_{oo}, \\ \dot{m} C_s T_{ist} + Q_{St} &= \dot{m} C_s T_{ost}, \\ Q_{St} &= U_{St} A_{St} LMTD_{St}, \end{aligned} \tag{7.7}$$

that form a system of three equations and three unknowns. The unknowns are the outlet oil and outlet salt temperatures, T_{oo} and T_{ost} respectively, and the heat exchanged Q_{St}. The value of the product of the thermal transmittance U_{St} and the exchange area A_{St} has been obtained by following the method explained in [11]. This value is 159.65 kJ/s °C.

7.3 CONTROL STRATEGIES

In this section two control strategies are presented. The first one consist of a PI controller followed by a series feedforward that manipulates the total oil flow through the field $\dot{q}_t$ in order to keep constant the outlet oil temperature; and another PI that manipulates the storage oil flow $\dot{q}_a$ to maintain the reference value of electrical power. The second one consists of a MPC controller that manipulates the same variables than the other strategy but it is aimed at keeping the reference value of electrical power while maximizing the thermal energy stored.

7.3.1 Constant Temperature

This strategy is similar to the one used in commercial plants, in which the outlet oil temperature of the field is kept constant to a value close to the maximum allowable one (usually around 390°C) due to oil degradation. Therefore, a PI followed by a series feedforward is used (figure 7.2). This control scheme is the same one used in [4] and [9] with a change in their parameters value due to the change of the field and the power cycle. The new PI controller has a gain of 0.7 °C/°C and an integral time of 300 seconds (these new values has been obtained using the method explained in [9]), while the new feedforward has the following expression

$$\dot{q}_t = \frac{5.561I - 4.149(u - 157.46) - 596.982}{u - Tin}. \tag{7.8}$$

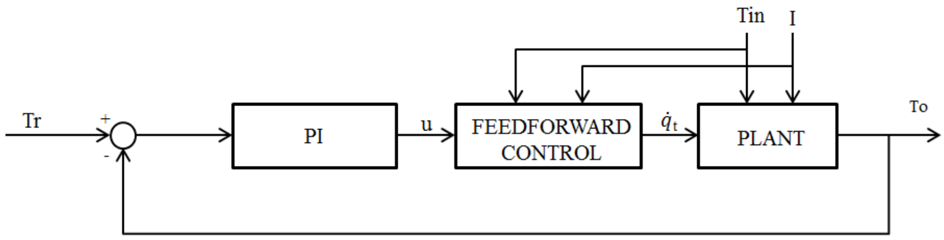

Figure 7.2: PI followed by a series feedforward

In this strategy the electrical power is also controlled with a PI controller that manipulates the storage oil flow $\dot{q}_a$. The reference value is 1200kW and the controller has a gain of 0.01 kg/(s kW) and an integral time of 100 seconds. This second controller interacts with the temperature controller. If $\dot{q}_a$ changes, the outlet oil temperature leaving the storage system will change, producing in turn a change in the inlet oil temperature. This change of the inlet temperature is a disturbance for the temperature controller, which will have to change the value of $\dot{q}_t$ to reject the disturbance; however, this change is a disturbance for the electrical power, which will have to change the value of $\dot{q}_a$, and so on, until a new steady state is reached. For that reason, an analysis of the degree of interaction between them has been made using the Relative Gain Array. The RGA obtained for this system was:

$$\begin{bmatrix} 1.11 & -0.11 \\ -0.11 & 1.11 \end{bmatrix}$$

that means that the diagonal pairing, which is the one chosen in this case, is the recommended one. In addition, due to the fact that its value is nearly one, it can be assumed that the interactions will be negligible. Nevertheless, the RGA give information about the steady state, and therefore, to be sure that the interactions are negligible for all the frequencies it is necessary to calculate the frequency-dependent RGA. In this case, as can be seen in figure 7.3, the value of the diagonal pairing (the one with a value of 1.11 in the RGA matrix) is also around one for all the frequencies, whereas the off-diagonal pairing (the one with a value of -0.11 in the RGA matrix) is below the value of 0. Therefore, it can be assumed that the interactions are negligible for all the frequencies.

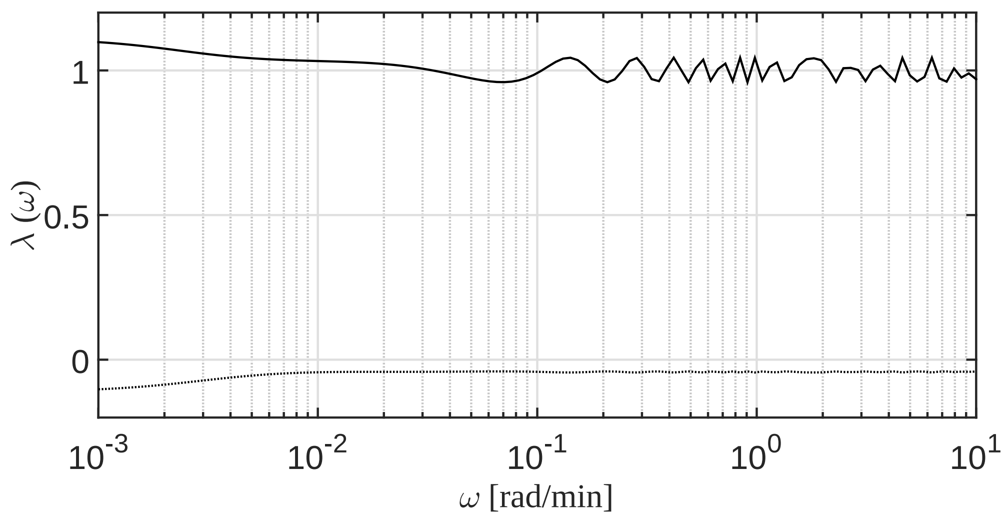

Figure 7.3: Frequency-dependent RGA

7.3.2 MPC

This control strategy consist of a MPC controller that uses models of the field, the power cycle, and predictions of the passing clouds through the field, so that the controller calculates the optimum value of total oil flow through the solar field $\dot{q}_t$ and the storage oil flow $\dot{q}_a$ that maximizes the thermal energy stored and maintain the electrical power at its set point. The solar collector field model used by the MPC is a simplification of the one used to simulated the real field, which assumes that the pipe is only divided in 6 parts of 80 meters instead of the divisions of 1 meter for passive zones and 3 meters for the active zones. The prediction of the passing clouds has been made assuming that the exact position of the cloud is known for each sampling interval of the prediction horizon, although the value of the incident solar radiation is supposed to be constant for each sampling interval, which adds some degree of error between the predicted value and the real one. The control structure can be seen in figure 7.4.

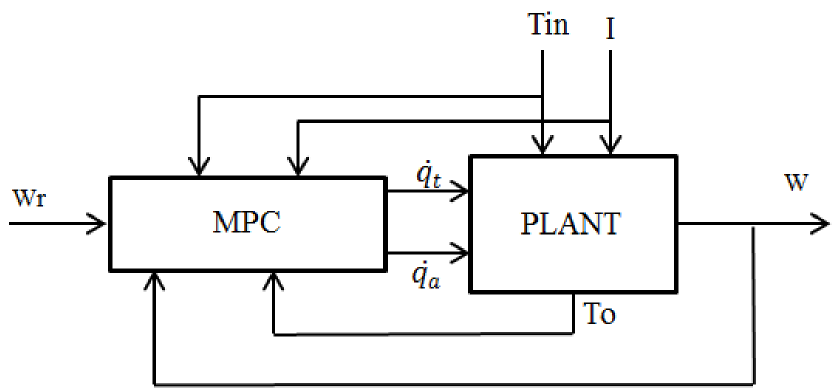

Figure 7.4: MPC controller

The thermal energy stored and the error between the power reference and the controlled variable are considered along an extended period of time, from time $(k+1)h$ up to some horizon $(k+H)h$, where k denotes present discrete time, H is the prediction horizon, and h is the sampling interval, which in this case has a value of 39 seconds. Therefore, the aim is to select the values of $\dot{q}_t$ and $\dot{q}_a$ that minimizes the multistep cost function

$$J = \sum_{i=1}^{H}[\lambda_1(W_r - W_i)^2 + \lambda_2(\Delta\dot{q}_t)^2 + (TL + W_{pump})], \tag{7.9}$$

subject to

$$\begin{aligned} T &\leq 400°C \\ 0.133 l/s \leq \dot{q} &\leq 1.58 l/s \\ 0 kg/s \leq \dot{q}_a &\leq \dot{q}_t kg/s \end{aligned}$$

where W_r is the reference value, W_i is the electrical power produced by the turbo-generator, TL are the thermal losses of the solar field, and W_{pump} is the electrical power consumed by the pump. Therefore, the minimization of J allows to maximize the thermal energy collected by the solar collector field (a direct consequence of minimizing the sum of the thermal losses and the consumption of the pump), that in turns implies that the maximum thermal energy is stored while keeping the reference value of the electrical power produced (minimizing the quadratic error between W_r and W_i), as can be deduced by studying the scheme of how the solar energy collected by the field is distributed, presented in figure 7.5. In addition a term taking into account the variations in the variable $\dot{q}_t$ is included in order to avoid sudden changes. The parameters λ_1 and λ_2 are weighting sequences. The maximization of J is performed with a receding horizon strategy, using a prediction horizon of H=12 and a control horizon of 3 [12].

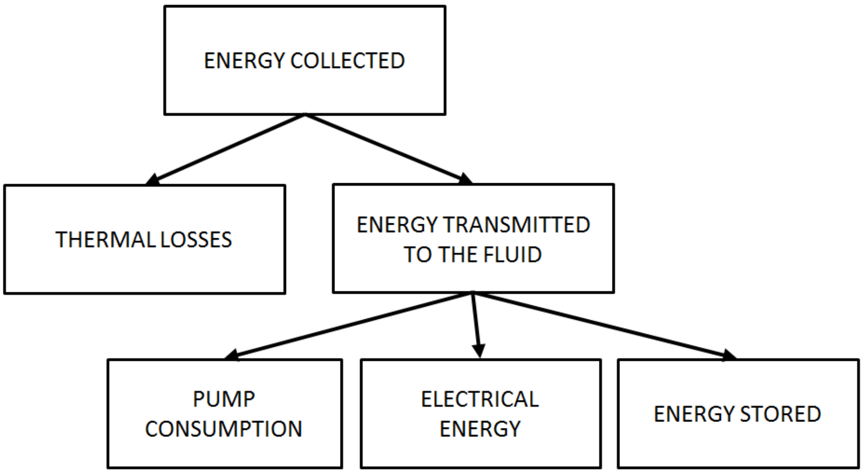

Figure 7.5: Distribution of the solar energy collected by the field.

The optimization is subject to restrictions in each loop oil outlet temperature ($T \leq 400°$C), oil flow (0.133 $l/s \leq \dot{q} \leq 1.58$ l/s), and in the oil flow sent to the storage system (0 $kg/s \leq \dot{q}_a \leq \dot{q}_t$ kg/s). The optimization is carried out for each integration step by the function $fmincon$ in MATLAB. The optimum values of $\dot{q}_t$ and $\dot{q}_a$ are then sent as the new set points of the flow controllers, which manipulate the variable frequency drives. In this simulation, the dynamics of the flow controllers plus the dynamics of the pumps and the hydraulic circuit are assumed to be like a second order system.

7.4 SIMULATION RESULTS

This section shows the results obtained by simulations of both control strategies explained in the previous section, especially during days with partial radiation, that is, when different parts of the solar field receive different degrees of solar radiation. In this paper four different cases have been studied, each one with a different degree of partial covering of the field. The first three have the same size of the passing clouds, but different times of passage; whereas, the last case was simulated using a real solar radiation curve. The reference value of the electrical power W_{ref} is 1200 kW, and the values of λ_1 and λ_2 of the MPC controller are 1 and 0 respectively for all the simulations. The first case consists of a day without clouds so that it could be used as a reference. The incident solar radiation curve used in this case can be seen in figure 7.6. The electrical power produced by both control strategies can be seen in figure 7.8, where it is clear that the MPC controller can maintain the production required during an extended period of time with less deviation from the reference value. This advantage is due to the fact that the MPC can change the value of the operating temperature depending on the value of the solar radiation [11]. In addition the MPC is capable of storing a high amount of thermal energy, as can be seen in figure 7.10, as a result of the same reason explained before. Finally, in figure 7.9 it is clear how the constant temperature strategy has to lower the oil flow almost to its minimum value when the value of the solar radiation is low in order to maintain its temperature set point, while the MPC presents a nearly constant value of oil flow. The improvement achieved by the MPC strategy in this case and in the following ones is shown in table 7.2, where the improvement refers to the percentage of more hours achieved during the operation of the field, the use of the stored energy for producing the demanded electrical power when the solar field operation is over, and the total number of hours of production.

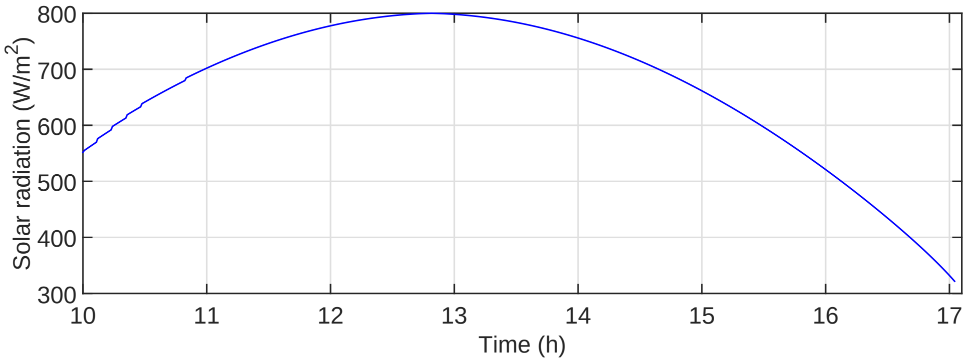

Figure 7.6: Average incident solar radiation

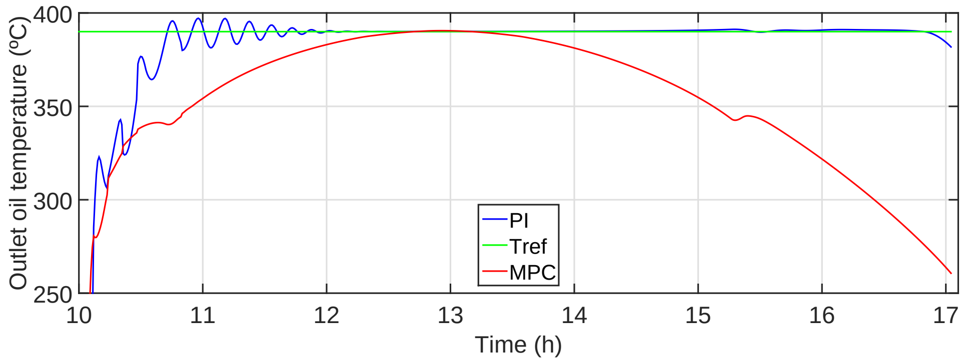

Figure 7.7: Oil outlet temperature of the field obtained with the constant temperature and MPC strategies

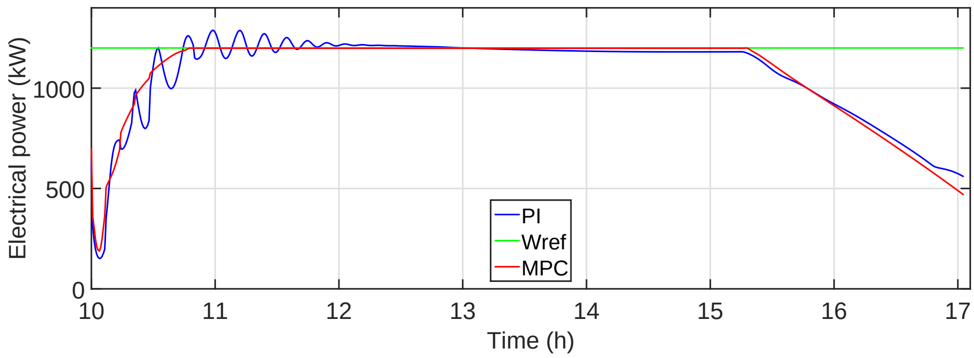

Figure 7.8: Electrical power generated by the constant temperature and MPC strategies

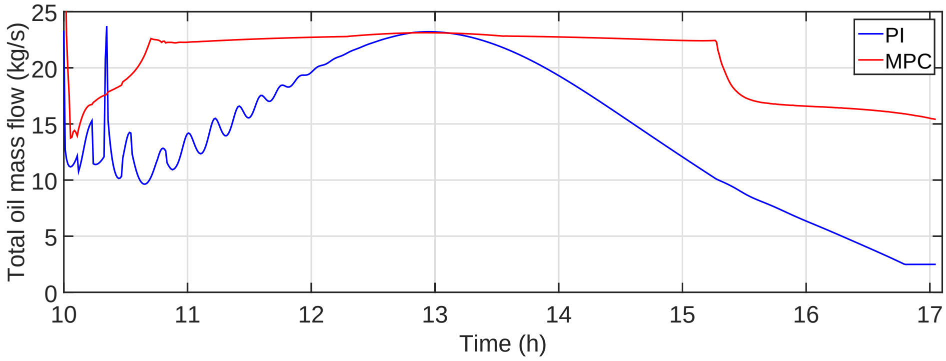

Figure 7.9: Total oil mass flow with the constant temperature and MPC strategies

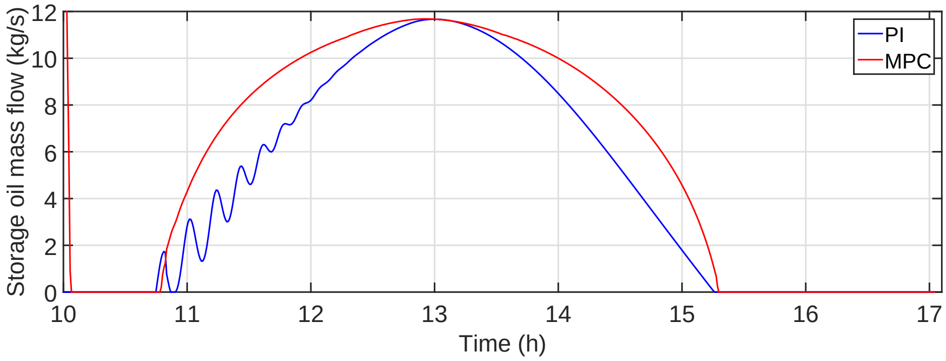

Figure 7.10: Storage oil mass flow with the constant temperature and MPC strategies

Table 7.2: Percentage of improvement achieved with the MPC strategy

Time of passage	% Operation	% Stored energy	% Total production
No clouds	1.09	16.52	4.1
45	8.33	20.44	10.64
15	2.27	11.29	3.73
Real data radiation curve	30.61	-6.44	24.2

The second and third cases use the same solar radiation curve with the addition of the passage of clouds. These passing clouds have been simulated with the model described in section 2 with the following parameters: a size of 16x16, a velocity of 2 matrix elements per integration step, a direction of 45°, an attenuation factor of 0, and a time of passage of 45 and 15 respectively. This time of passage has been defined as the number of integration steps where there is no cloud over the field after the last one had abandoned it; this criteria means that during all the simulation there are passing clouds entering and leaving the field, separated by this time. The solar radiation curve including the passage of the clouds is shown in figure 7.11. It is necessary to clarify that this curve shows the average solar radiation reaching the field, not the solar radiation reaching each loop, that depends on the passing clouds model. The performance of both control strategies for the second case can be seen in figures 7.12, 7.13, 7.14, and 7.15. Compared with the first case, it is clear that the presence of clouds at the end of the day results in a lower period of time of electrical power production for the constant temperature strategy. However, the MPC strategy can produce the required electrical power for around the same period of time as the first case, and therefore in table 7.2 can be seen a higher improvement in both the operation and the stored energy.

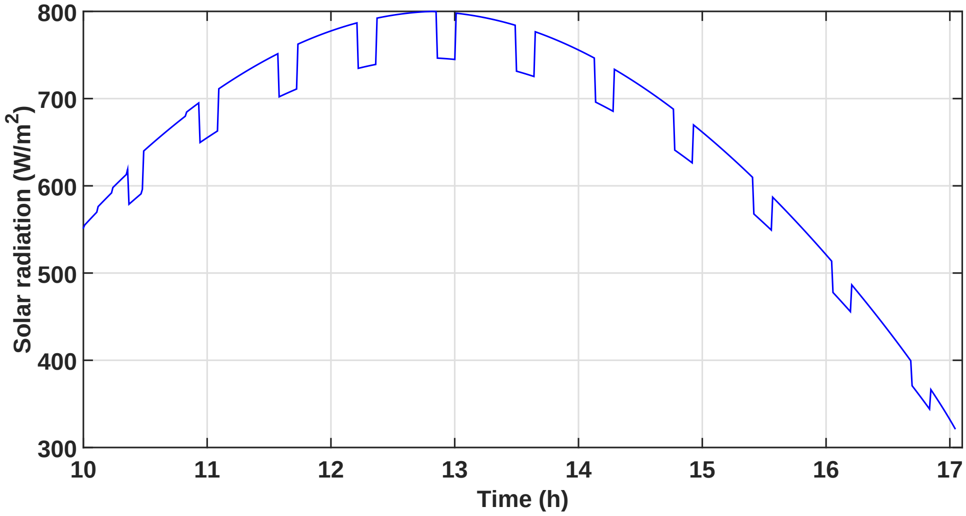

Figure 7.11: Average incident solar radiation

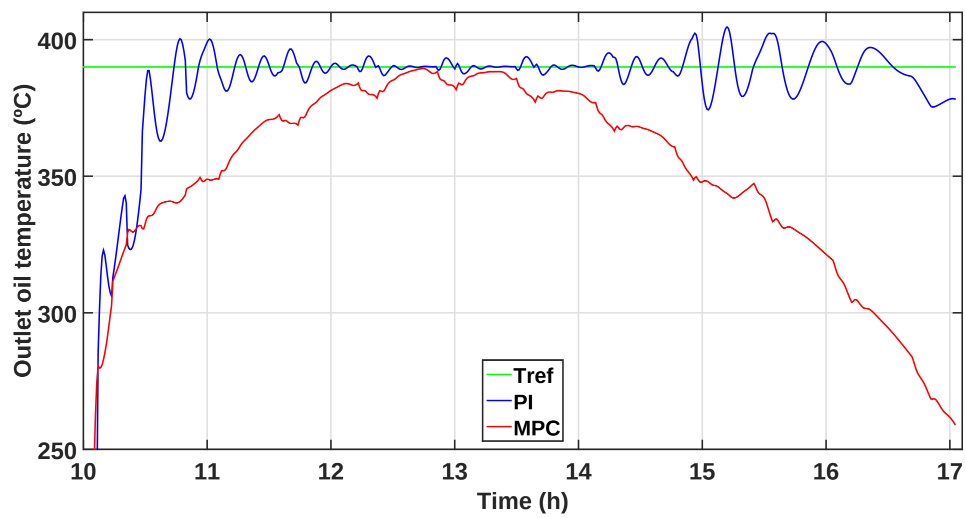

Figure 7.12: Oil outlet temperature of the field obtained with the constant temperature and MPC strategies

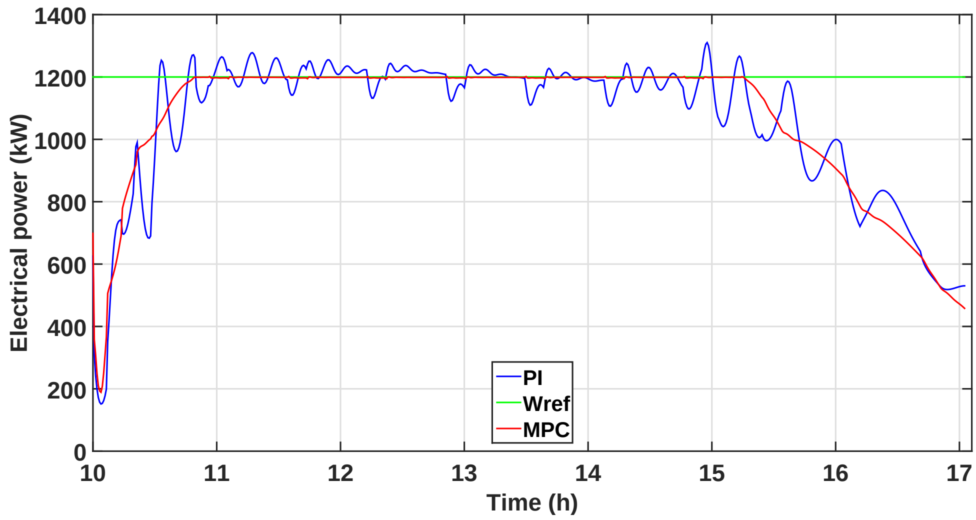

Figure 7.13: Electrical power generated by the constant temperature and MPC strategies

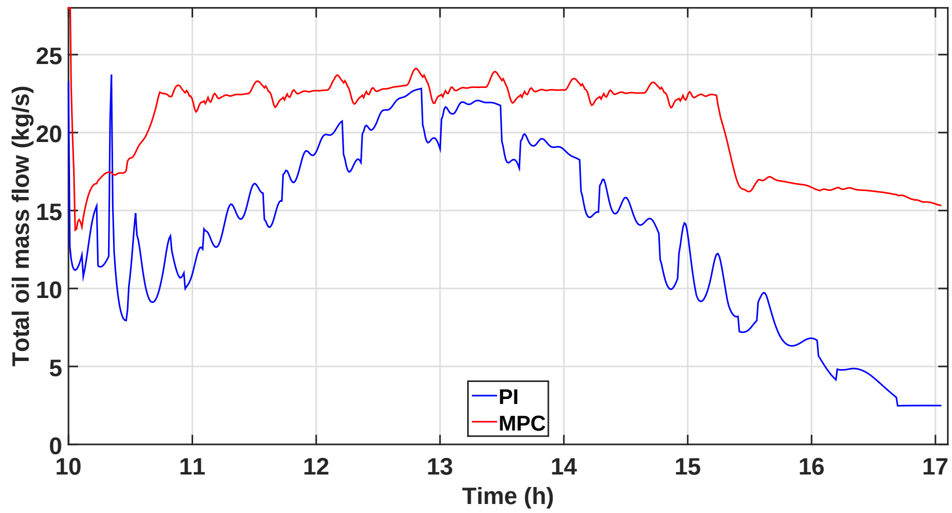

Figure 7.14: Total oil mass flow with the constant temperature and MPC strategies

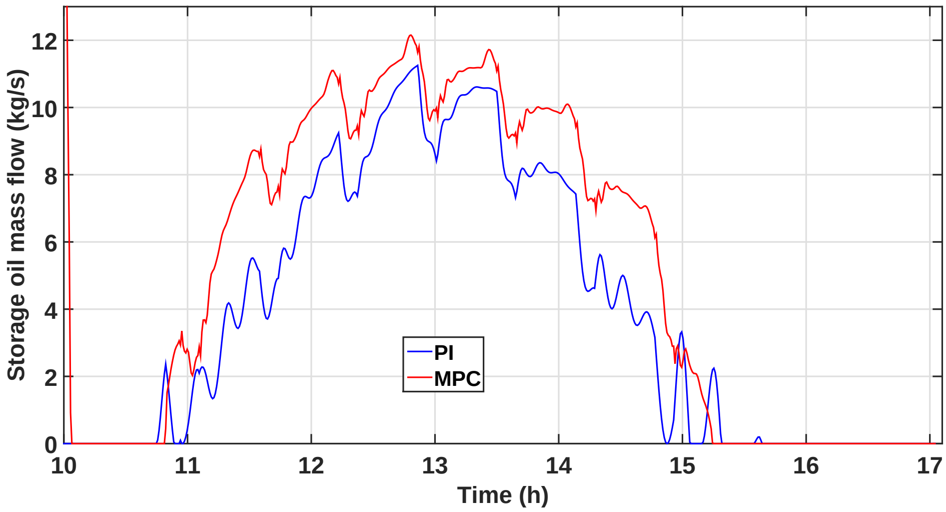

Figure 7.15: Storage oil mass flow with the constant temperature and MPC strategies

The third case is similar to the second one, but with a decrease in the time of passage from 45 to 15 (figure 7.16). This new time of passage implies that there are more clouds passing over the field along the day and that this disturbance has a higher frequency. For that reason, if the constant temperature strategy continues working with an outlet oil temperature reference of 390°C, the problem of the appearance of temperature peaks in some of the loops happens. Therefore, in order to avoid this problem, a new temperature reference of 380°C was used. A more detailed explanation of this problem can be found in [10]. The performance of both control strategies for this case is shown in figures 7.17, 7.18, 7.19, and 7.20. It is clear that in this case the MPC strategy remains the one that produces electrical power for a longer period of time and stores a higher amount of thermal energy as can be seen in table 7.2. Nevertheless, due to the decrease in the outlet oil temperature reference for the constant temperature strategy the production time of the electrical power has been extended compared with the case which would have a higher temperature reference, and that is the reason why the percentage of improvement of the operation (table 7.2) is less than in the second case despite having a higher presence of clouds. In addition, the value of thermal energy stored is lower with both strategies due to the fact that there is less excess of energy to be stored, and so, the percentage of improvement of the stored energy is lower.

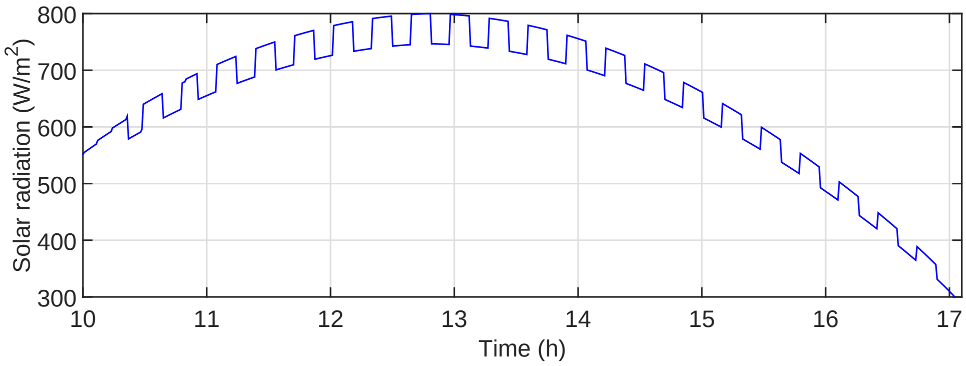

Figure 7.16: Average incident solar radiation

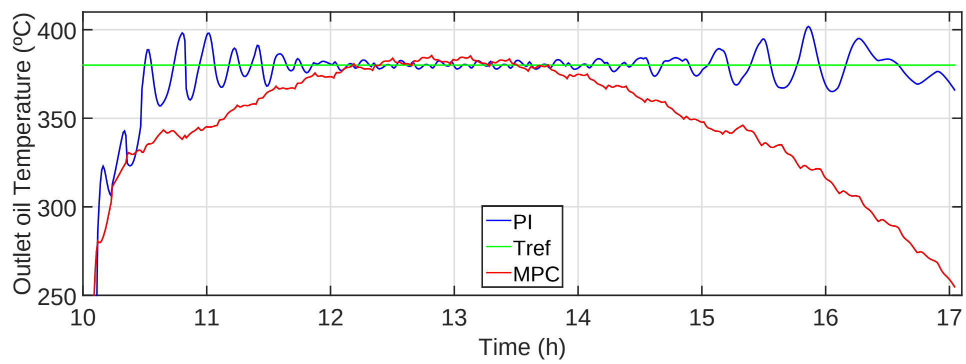

Figure 7.17: Oil outlet temperature of the field obtained with the constant temperature and MPC strategies

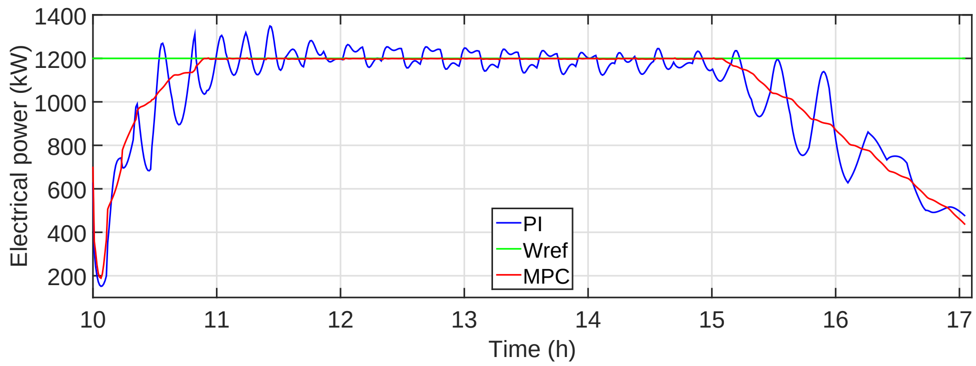

Figure 7.18: Electrical power generated by the constant temperature and MPC strategies

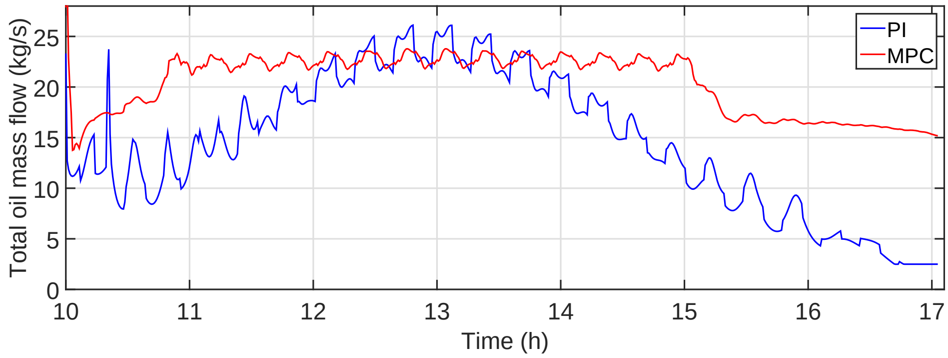

Figure 7.19: Total oil mass flow with the constant temperature and MPC strategies

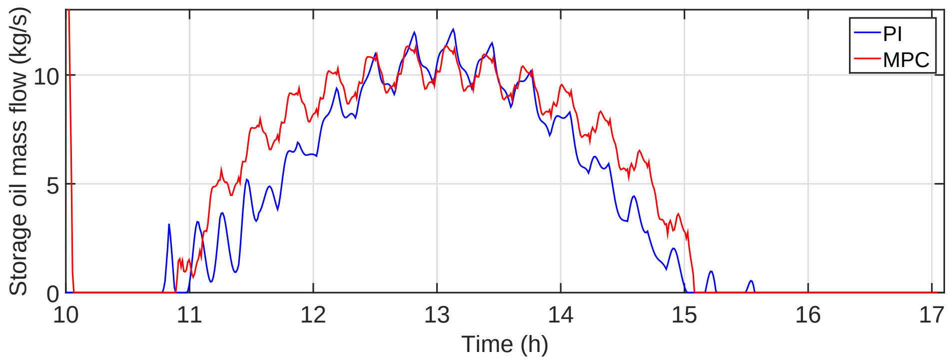

Figure 7.20: Storage oil mass flow with the constant temperature and MPC strategies

Finally, the fourth case consists of a solar radiation curve made with real data (figure 7.21) and affects all loops equally instead of having a different degree of radiation affecting each loop as was the situation of the cases described before. In addition the MPC does not use predictions of the clouds in this case. The performance of both strategies is shown in figures 7.22, 7.23, 7.24, and 7.25. In this case the level of solar radiation is so irregular that the MPC strategy achieves a great improvement in the operation, but at the cost of storing less thermal energy. However the improvement in the total production is the highest one of the five cases. This is due to the higher value of electrical power production coming from the operation of the field rather than stored energy.

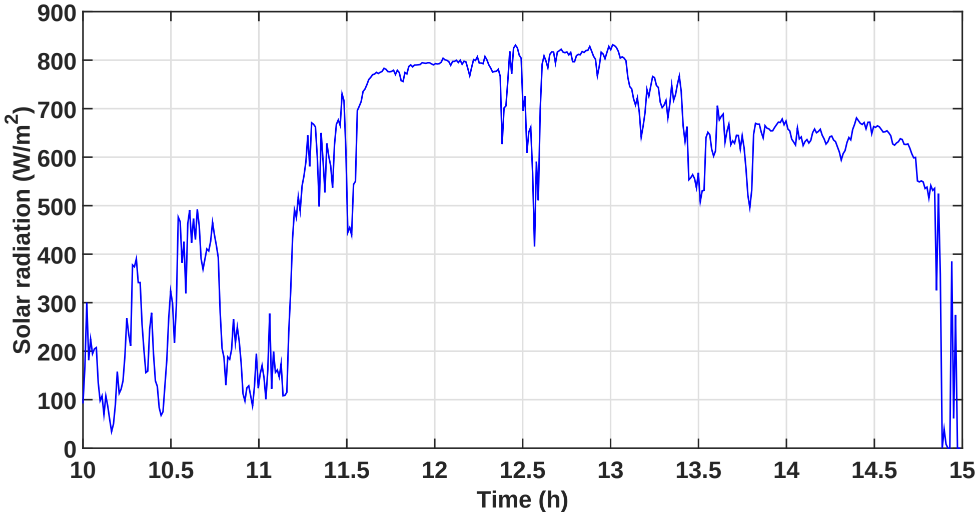

Figure 7.21: Average incident solar radiation

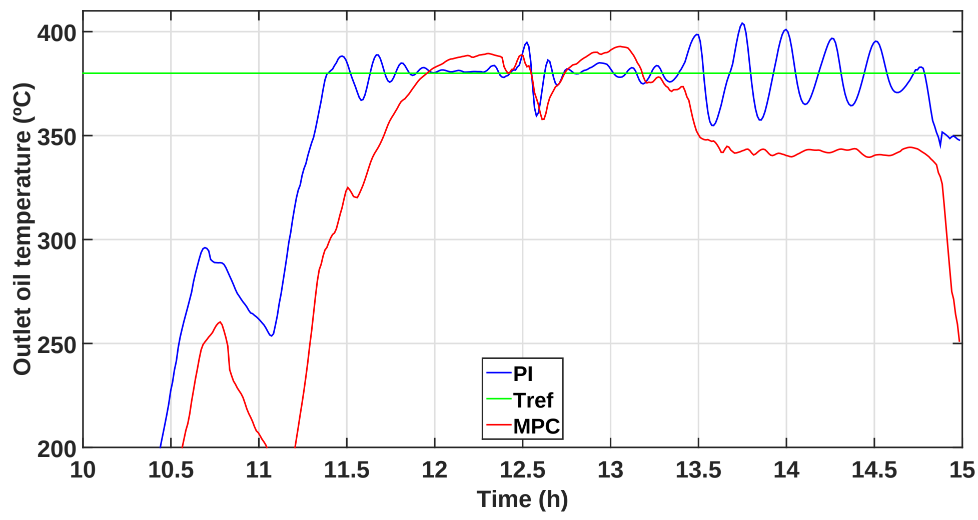

Figure 7.22: Oil outlet temperature of the field obtained with the constant temperature and MPC strategies

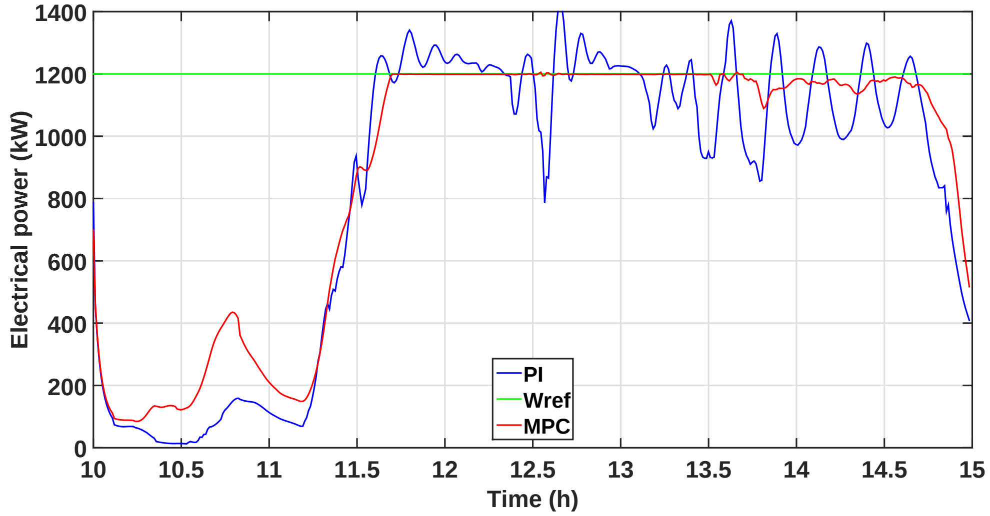

Figure 7.23: Electrical power generated by the constant temperature and MPC strategies

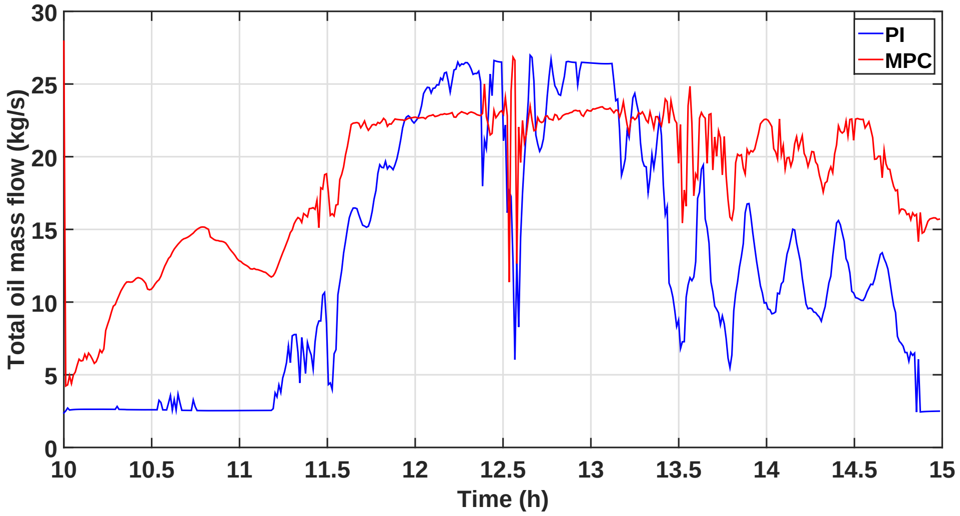

Figure 7.24: Total oil mass flow with the constant temperature and MPC strategies

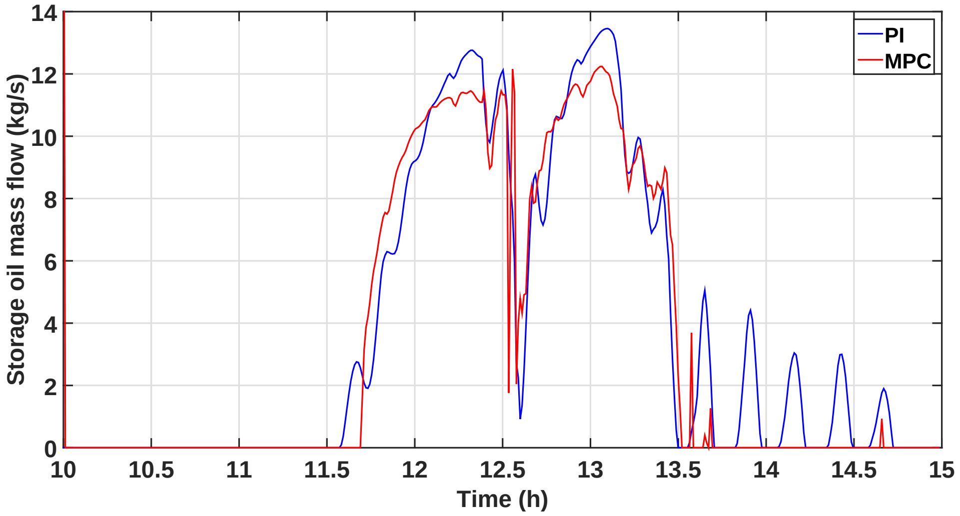

Figure 7.25: Storage oil mass flow with the constant temperature and MPC strategies

7.5 CONCLUSIONS

The main conclusion of this paper is that the MPC strategy improves the number of hours of electrical power production of the plant and also the amount of thermal energy stored in the molten salts storage system, compared to a control strategy that uses a constant value of temperature. This improvement increases when the solar collector field is affected by solar radiation disturbances produced by the passage of clouds, however, the increase depends on the time of passage and the size of the clouds, varying from 4% to 12%. In addition, with the MPC controller a better controllability of the electrical power generated is achieved, being less affected by the disturbances, which in turns reduces the economic penalties for deviating from the reference electrical power value.

Bibliography

[1] Abutayeh, M., Alazzam, A. and El-Khasawneh, B. (2014). *Balancing heat transfer fluid flow in solar fields.* Solar Energy, 105, 381-389.

[2] Al-Maliki, W. A. K., Alobaid, F., Starkloff, R., Kez, V. and Epple, B.(2016). *Investigation on the dynamic behaviour of a parabolic trough power plant during strongly cloudy days.* Applied Thermal Engineering, 99, 114-132.

[3] Boukelia, T. E., Arslan, O. and Mecibah, M. S. (2016). *ANN-based optimization of a parabolic trough solar thermal power plant.* Applied Thermal Engineering, 107, 1210-1218.

[4] Camacho, E. F., Berenguel, M. and Rubio, F. R. (1997). *Advanced control of solar plants.* Springer-Verlag, London.

[5] Camacho, E. F., Berenguel, M., Rubio, F. R. and Martínez, D. (2012). *Control of solar energy systems.* Springer-Verlag, London.

[6] Camacho, E. F., Berenguel, M. and Gallego, A. J. (2014). *Control of thermal solar energy plants.* Journal of Process Control, Vol.24-2, 332-340.

[7] Carmona, R., (1985). *Análisis, modelado y control de un campo de colectores solares distribuidos con sistema de seguimiento en eje.* Ph.D. Thesis.

[8] Lippke, F. (1995). *Simulation of the part-load behavior of a 30 MWe SEGS plant.* Report No. SAND95-1293, SNL, Albuquerque, NM, USA.

[9] Navas, S. J., Rubio, F. R., Ollero, P. and Ortega, M. G. (2016). *Modeling and simulation of parabolic trough solar fields with partial radiation.* XV European Control Conference, 31-36.

[10] Navas, S. J., Rubio, F. R. and Ollero, P. (2017). *Optimum control of parabolic trough solar fields with partial radiation.* IFAC-PapersOnLine, Vol.50-1, 109-114.

[11] Navas, S. J., Ollero, P. and Rubio, F. R. (2017). *Optimum operating temperature of parabolic trough solar fields.* Solar Energy, 158, 295-302.

[12] Navas, S. J., Rubio, F. R., Ollero, P. and Lemos, J. M. (2018). *Optimal control applied to distributed solar collector fields with partial radiation.* Solar Energy, 159C, 811-819.

[13] Rubio, F. R., Camacho, E. F. and Berenguel, M. (2014). *Control of solar collector fields.* Revista Iberoamericana de Automática e Informática Industrial (RIAI), 3-4, 26-45.

[14] Smith, R. (2005). *Chemical process design and integration.* Wiley.

Chapter 8

Congress Paper

Optimum Control of Parabolic Trough Solar Fields with Partial Radiation
Sergio J. Navas, Francisco R. Rubio, and Pedro Ollero. IFAC-PapersOnLine. Volume 50 (1), 2017. DOI:https://doi.org/10.1016/j.ifacol.2017.08.019

This paper describes the main problems of operating parabolic trough solar fields during days with partial radiation. An optimal control strategy is proposed to solve these problems and it is assessed against a classical one, which uses a feedforward and a PI controller with a fixed set point of oil outlet temperature. Some simulations have been made using MATLAB to demonstrate that using the optimal control strategy better results can be achieved.

8.1 INTRODUCTION

The main technologies for converting solar energy into electricity are photovoltaic (PV) and concentrated solar thermal (CST). Parabolic trough, solar towers, Fresnel collector and solar dishes are the most used technologies for concentrating solar energy. This paper focus on parabolic trough solar fields, which consist of a collector field (Fig. 8.1), a power cycle and auxiliary elements such as pumps, pipes and valves. The solar collector field collects solar radiation and focuses it onto a tube in which a heat transfer fluid, usually synthetic oil, circulates. The oil is heated up and then used by the power cycle to produce electricity by means of a turbine.

The main goal of a parabolic trough solar field is to collect the maximum solar energy in order to produce as much electrical power as possible. Normally, this is achieved by keeping the outlet temperature of the field around the maximum allowable value, that is 400°C, due to oil degradation. However, in this paper, we will show that this way to operate the field does not produce the best results of electrical power generated. This problem has been studied before in [14], where it was suggested that the optimum strategy is based on adapting the fluid outlet temperature to the incident solar radiation, keeping the constant the superheating temperature of the steam; it was also studied in [15] where a constant outlet temperature was used (393°C). Finally, a more recent study was carried out in [7] where it was proposed to change the outlet temperature set point according to the value of the solar radiation.

On the other hand, using a PI with a feedforward controller that manipulates the oil flow to keep constant the outlet temperature of the field, like in [3]-[6]-[8], while a cloud is passing through the field may provoke temperature peaks in some loops. This situation is due to the fact that when the cloud passes the controller will decrease the oil flow in order to keep the outlet temperature constant, however, in the loops that are not covered by the cloud, the solar radiation is not reduced, so that their temperature will be increased above the security limit. If this situation happens the collectors are programmed to get out of focus to prevent oil degradation, but that would involve a loss of energy and it is not considered in this paper as a possible solution.

In this paper the effect of the solar radiation on the outlet temperature was studied with a complete power cycle model (Fig. 8.2) reduced to a correlation that relates the electrical power generated by the condensation turbine with the mass flow and outlet temperature of the oil. In [7] it is used a similar approach but they use a correlation that only depends on the outlet temperature, that implies efficiency results higher than the ones found in the literature [14]; in addition the simulations made in this paper were carried out taking into account a model of the entire field, not assuming that the behavior of one loop is the same than the other ones. Therefore, the authors propose that using an optimal controller with constraints can prevent the appearance of temperature peaks and also maximize the electrical power generated by the field depending on the value of solar radiation.

The paper is organized as follows: Section 2 describes the models of the solar field, passing clouds and power cycle used for simulation purposes. Section III describes both control strategies tested: the feedforward with a PI control and the optimum control. Section IV shows the results obtained by simulations made in MATLAB. Finally, the paper draws to a close with some concluding remarks.

Figure 8.1: ACUREX distributed solar collector field

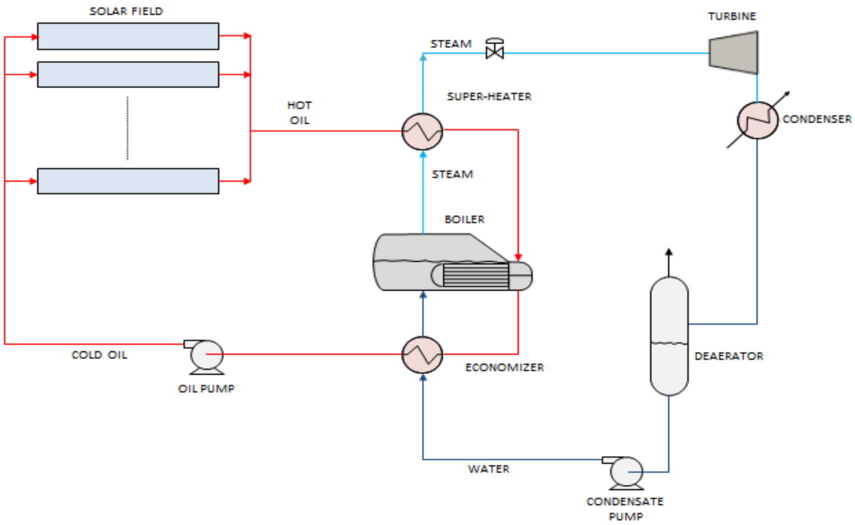

Figure 8.2: Diagram of the solar field connected with the power cycle

8.2 SYSTEM MODELING

The model of each of the parts which have been used to simulate the operation of a solar field during the days with partial covering is presented. These parts are: the solar collector field, the passage of the clouds and the power cycle.

8.2.1 Solar Collector Field Model

In this subsection, the mathematical model of a parabolic trough solar field is presented. This model is the same used in [16] which is at the same time a slight modification of the model proposed by [3]-[6]-[8] for the ACUREX field (Fig. 8.1). Basically, this model can be used to simulate parabolic trough solar fields by selecting parameters like the number of active (the parts where the solar radiation reaches the tube) and passive (joints and other parts not reached by concentrated solar radiation) zones, length of each zone, or collector aperture. The solar field simulated in this paper is supposed to be on the site of the Escuela Superior de Ingeniería de Sevilla. It is composed of 24 loops and has dimensions of 144x240 m^2. Each loop is modeled by the following system of partial differential equations describing the energy balance:

Active zones

$$\rho_m C_m A_m \frac{\partial T_m}{\partial t} = I n_0 G - H_l G (T_m - T_a) - LH_t (T_m - T_f) \tag{8.1}$$

Fluid element

$$\rho_f C_f A_f \frac{\partial T_f}{\partial t} + \rho_f C_f \dot{q} \frac{\partial T_f}{\partial x} = LH_t (T_m - T_f) \tag{8.2}$$

Passive zones

$$\rho_m C_m A_m \frac{\partial T_m}{\partial t} = -H_p (T_m - T_a) - LH_t (T_m - T_f) \tag{8.3}$$

where the sub-index m refers to metal and f refers to the fluid. The model parameters and their units are shown in table 8.1.

Table 8.1: Solar field model parameters description

Symbol	Description	Units
t	Time	s
x	Space	m
ρ	Density	Kg/m^3
C	Specific heat capacity	J/(K kg)
A	Cross sectional area	m^2
T	Temperature	°C
$\dot{q}$	Oil flow rate	m^3/s
I	Solar radiation	W/m^2
n_0	Optical efficiency	Unit-less
G	Collector aperture	M
T_a	Ambient Temperature	°C
H_l	Global coefficient of thermal losses for active zones	W/(m^2 °C)
H_t	Coefficient of heat transmission metal-fluid	W/(m^2 °C)
H_p	Global coefficient of thermal losses for passive zones	W/(m^2 °C)
L	Length of pipe line	m

The density ρ, specific heat C and coefficient of thermal loss H_l depend on fluid temperature. The coefficient of heat transmission H_t depends on temperature and oil flow. The incident solar radiation I depends on hourly angle, solar hour, declination, Julianne day, local latitude and collector dimensions [3]-[6]-[8]. In order to solve this system of partial differential equations, a two stage finite difference equation has been programmed, considering each segment of 1 m for the passive zones and of 3 m for the active zones and solving (8.1)-(8.2)-(8.3).

8.2.2 Modeling of the Passing Clouds

The modeling of the passing clouds is necessary to know how the radiation of the sun is distributed throughout the field. This can be achieved creating a matrix which represents the whole field extension. Each element of the matrix is assigned the value of the incident solar radiation on that section at each time. The solar field has dimensions of 144x240 m^2, so if we divide the matrix in elements of 3x3 meters we need a 48x80 matrix. The matrix is then put over the field in such a way that each element contains a fraction of an active or passive element. Fig.8.3 shows the fraction of the whole matrix that covers one loop of a generic field.

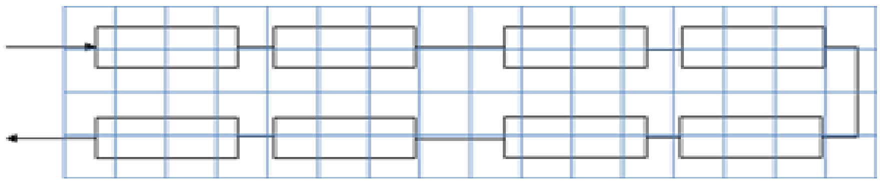

Figure 8.3: Example of a fraction of the matrix over one loop of the field

The value of the radiation in each element of the matrix depends on the following parameters:

- The global incident solar radiation on the field.
- The direction of the route followed by the passing cloud (the angle formed by this direction and the direction followed by the thermal fluid, the parallel being 0).
- The velocity of the passing cloud (determined by the number of elements of the matrix supposed to be traveled by the cloud every 39 seconds, which is the sample time of the field).
- The size of the cloud (a rectangular form is supposed, defined by the rows and columns that it covers).
- The attenuation factor, which is the value that multiplies the radiation in the zones where the cloud is present. This value varies between 0 and 1 depending on the radiation which the cloud allows to arrive to the field, being 0 the case in which no radiation arrives to the field and 1 the case in which all the radiation arrives to it.

Once these values are set, the program calculates for each collector the mean value of radiation of every element of the matrix related with it. This mean value is assigned to the variable I of (8.1).

8.2.3 Power Cycle Model

The power cycle model used in this paper (Fig. 8.2) consists of an economizer, a boiler and a super-heater followed by a turbine. The oil flow heated by the solar radiation concentrated by field collectors is firstly introduced into the super-heated where a steam stream is heated. Afterward, the oil is used to produce saturated steam in the boiler, which operates at a floating pressure. Finally the oil is sent to the economizer to preheat the water stream before being boiled. The super-heated steam is used to produce electrical power in a condensation turbine.

This model was simulated using the software Engineering Equation Solver and then correlated with simulation results to get equations (8.4) and (8.5) in order to calculate the electrical power generated and the oil temperature returning to the field respectively. This simplification was necessary to reduce the simulation time and the error is around 1%. In addition the dynamic of the cycle was assumed to be like a first order model with a time constant of 100 seconds.

$$\begin{aligned} W = 8.23e^{3} - 49.96m_{oil} - 2.70m_{oil}^{2} - \\ 47.15T_{out} + 6.75e^{-2}T_{out}^{2} + 5.38e^{-1}m_{oil}T_{out} \end{aligned} \tag{8.4}$$

$$\begin{aligned} T_{in} = 3.40e^{2} + 1.78m_{oil} - 1.55e^{-1}m_{oil}^{2} - \\ T_{out} + 1.07e^{-3}T_{out}^{2} + 2.17e^{-2}m_{oil}T_{out} \end{aligned} \tag{8.5}$$

The net electrical power produced by the field is the result of subtracting the power consumed by the pump to the power generated by the turbine. Therefore, to calculate the consumption of the pump we used the Darcy equations. Firstly, the Reynolds number and the Barr's friction coefficient are computed by (8.6) and (8.7) respectively:

$$Re = \frac{\rho_f q d}{A_f \mu} \tag{8.6}$$

$$f = 0.25 \frac{1}{log10(\epsilon_r/3.7d + 5.74/Re^{0.9})^2} \tag{8.7}$$

where μ is the dynamic viscosity and ϵ_r is the relative rugosity. The Darcy equation for computing the pressure drop is given by (8.8):

$$hpl = 9806.65 \frac{8fLq^2}{g\pi^2 d^5}(Pa) \tag{8.8}$$

where L is the loop length and d is the pipe diameter. The power consumption depends on the pump efficiency, oil flow and the pressure drop pd (8.9).

$$W_{pump} = \frac{qhpl}{\eta_{pump}}(W) \tag{8.9}$$

Finally, the net electrical power is calculated by (8.10).

$$W_{net} = W - \frac{W_{pump}}{1000}(kW) \tag{8.10}$$

8.3 CONTROL STRATEGIES

In this section two control strategies are presented. The feedforward with PI control strategy is the traditional one used in solar fields to keep constant the oil outlet temperature, whereas the Optimal control strategy is a new one proposed by the authors in order to maximize the electrical power generated and prevent the appearance of temperature peaks.

8.3.1 Feedforward with PI Control

This control strategy consists of controlling the outlet temperature of the field by manipulating the total flow of the oil. This total flow is equally distributed among the loops. The control scheme can be seen in Fig. 8.4, where a series feedforward compensation is used.

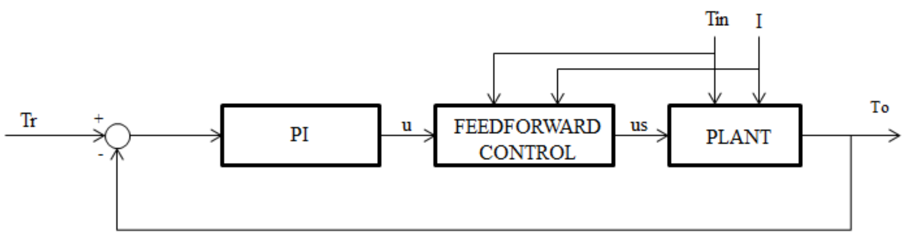

Figure 8.4: Series feedforward controller

The feedforward controller provides compensation for variations in I and T_{in} calculating the desired flow of oil u_s using (8.11), where T_0 is the outlet temperature to be maintained, Pc_p is a term that accounts for the product and quotient of characteristic magnitudes (areas, thermal capacities, etc.), S is the effective surface, H_l is the global thermal losses coefficient, and T_m is the mean inlet-outlet temperature. Equation (8.11) comes from the concentrated parameters model of the field [3]-[6]-[8] considering steady state conditions. This equation can be approximated by (8.12), where u is the output of a PI controller ($K_c = 1.09$, $\tau_i = 150.28\ s$) placed before the feedforward controller in order to maintain the required steady state outlet temperature T_0 due to the fact that exact compensation cannot be achieved with it.

$$(T_0 - T_{in})u_s = \frac{1}{Pc_p}(n_0 SI - H_l(T_m - T_a)) \tag{8.11}$$

$$u_s = \frac{3.15I - 0.204(u - 64.16) - 75.87}{u - T_{in}} \tag{8.12}$$

The radiation I used in (8.12) is the global incident solar radiation on the field which is calculated as the mean value of all elements of the matrix, and the variable T_{in} is the inlet temperature of the thermal fluid, calculated by (7.2). The constants that appear in the equation have been determined experimentally.

8.3.2 Optimal Control

This control strategy is based on using an MPC controller, which uses models of the field and the power cycle, so that the controller could calculate the optimum value of oil outlet temperature which maximizes the electrical power generated, taking into account temperature and oil flow constraints. The control scheme can be seen in Fig.8.5.The dynamic optimization procedure may be expressed as the following algorithm:

- All the variables needed by the field model are measured.
- A simplified solar collector field model (8.1)-(8.2), which assumes that the pipe is only divided in 6 parts of 80 meters instead of the divisions of 1 meter for passive zones and 3 meters for the active zones in the model used for simulating the solar field, is used to calculate the outlet oil temperature of the field. The oil flow is the independent variable used by the optimizer.

- With the calculated values of oil outlet temperature and mass oil flow, equations (7.1) and (7.2) are used to know the electrical power generated by the turbine and the inlet oil temperature.

- Finally, with equations (8.6), (8.7), (8.8), (8.9) and (8.10) the net electrical power is calculated.

Therefore, the MPC has to maximize the value of net electrical power subject to restrictions in oil temperature (T≤400°C) and oil flow (0.000133 m^3/s≤q≤0.00158 m^3/s) for each loop. The prediction and control horizons are equal to one, however, in future works, it is planned to increase these horizons incorporating predictions of the passing clouds. The optimization is carried out for each integration step by the function $fmincon$ in MATLAB. The optimum value of oil flow would be then sent as the new set point of the flow controller, which manipulates the variable frequency drive, but in this simulation we are assuming that the flow is instantly changed.

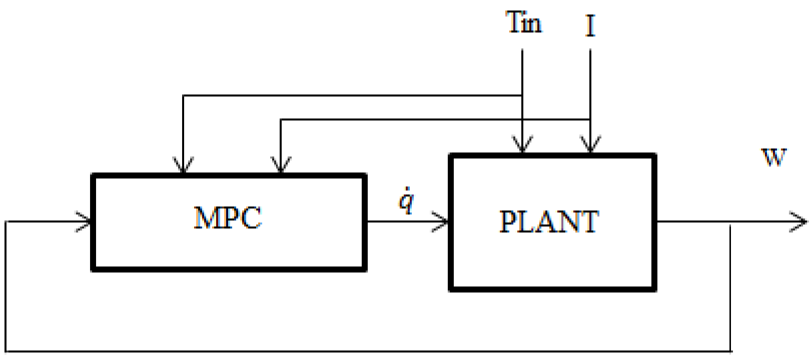

Figure 8.5: MPC controller

8.4 SIMULATION RESULTS

This section shows the results obtained by simulations of both strategies explained in Section 3. These simulations have been carried out with the solar radiation curve shown in (Fig. 8.6) and using the models described in section 2. If we compared the feedforward with PI strategy with a fixed set point of 393°C against the optimal one, we can see that the feedforward with PI strategy presents the problem of temperature peaks in some loops (Fig. 8.7) whereas in the optimal strategy this situation does not happen (Fig. 8.8).

The oscillations observed in Fig. 8.7 are due to use of a static feedforward with unmodelled dynamics; a problem that does not occur when the optimal controller is used (Fig. 8.8). In terms of electrical power (Fig. 8.9), it seems that during the central part of the day the feedforward strategy produces more than the optimal one, but at the cost of having temperature peaks. However, during the last part of the day, when the value of the incident solar radiation is low, the optimal strategy produces much more electrical power. Considering the entire operating day, the improvement achieved by the optimal strategy is around 2.15%.

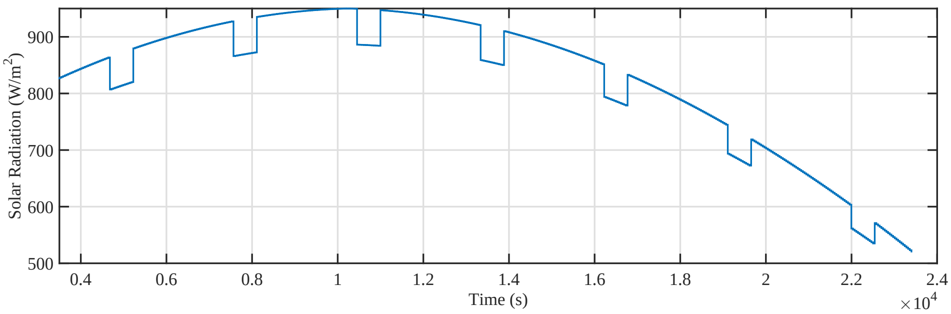

Figure 8.6: Incident solar radiation

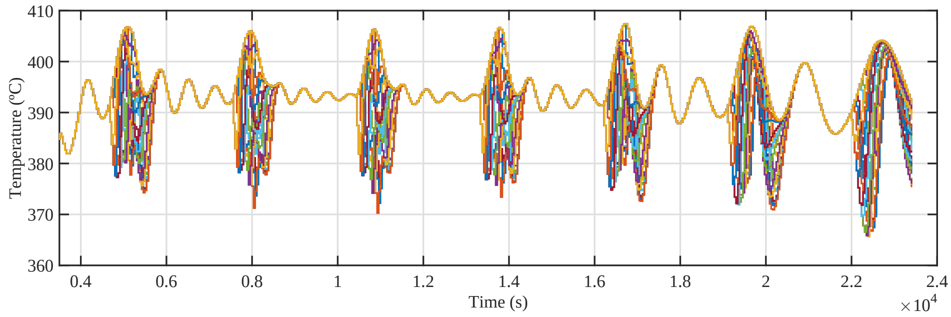

Figure 8.7: Oil outlet temperature of the loops with a feedforward controller and a set point of 393°C

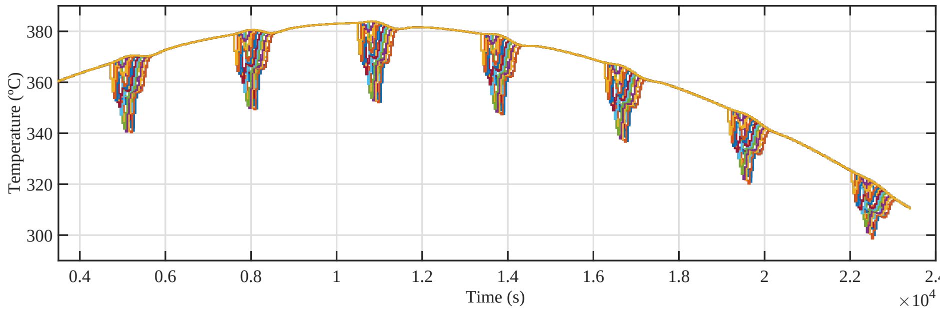

Figure 8.8: Oil outlet temperature of the loops with an optimal controller

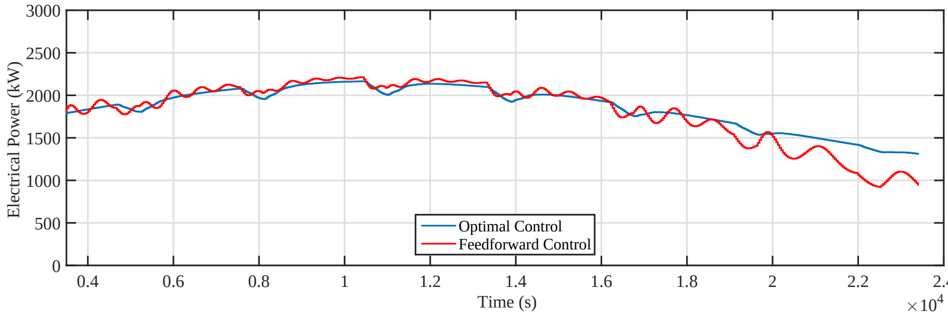

Figure 8.9: Electrical power generated by the optimal strategy and the feedforward strategy with a set point of 393°C

After seeing that with the feedforward with PI strategy with a set point of 393°C we could not avoid the problem of the appearance of temperature peaks, we tested the same strategy but with a lower set point equal to 380°C. Figure 8.10 shows that with this set point the temperature peaks do not appear, however, in terms of electrical power this new set point has worse results than the previous one (Fig. 8.11). Specifically, in this case the improvement achieved when compared with the optimal strategy is around 2.95%.

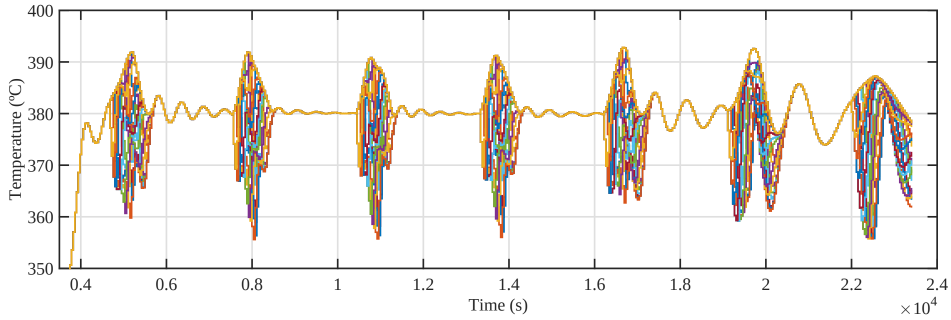

Figure 8.10: Oil outlet temperature of the loops with a feedforward controller and a set point of 380°C

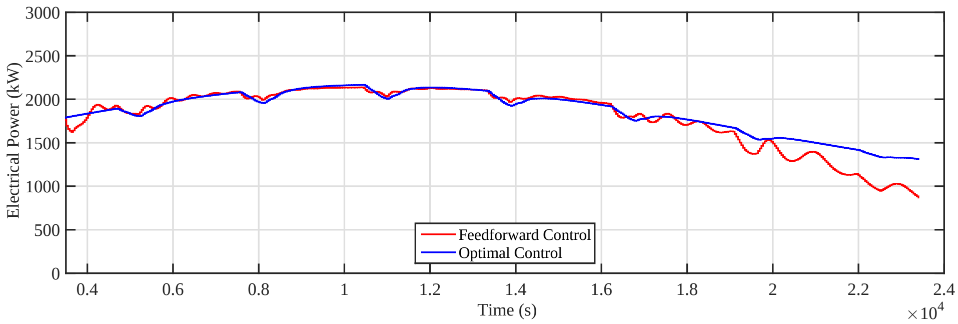

Figure 8.11: Electrical power generated by the optimal strategy and the feedforward strategy with a set point of 380°C

8.5 CONCLUSION

The main conclusion of this paper is, that to operate the field during a day with partial radiation at a constant oil outlet temperature is not the optimum way to do it and also can lead to the temperature peaks problem. Using the feedforward with PI strategy the only way to avoid this problem is to lower the oil outlet temperature set point, but in doing so, it also reduces the total amount of electrical power generated. For that reason the authors propose the use of the optimal strategy, which can prevent the temperature peaks problem and also maximizes the electrical power production, not only when there are passing clouds, but also when the value of the incident solar radiation is low.

Bibliography

[1] Abutayeh, M., Alazzam, A. and El-Khasawneh, B. (2014). *Balancing heat transfer fluid flow in solar fields.* Solar Energy, 105, 381-389.

[2] Barão, M., Lemos, J. and Silva, R. (2002). *Reduced complexity adaptive nonlinear control of a distributed collector solar field.* Journal of Process Control, 12-1, 131-141.

[3] Camacho, E. F., Berenguel, M. and Rubio, F. (1997). *Advanced control of solar plants.* Springer-Verlag, London.

[4] Camacho, E. F., Rubio, F. R., Berenguel, M. and Valenzuela, L. (2007). *A survey on control schemes for distributed solar collector fields. Part I: Modeling and basic control approaches.* Solar Energy, 81-10, 1240-1251.

[5] Camacho, E. F., Rubio, F. R., Berenguel, M. and Valenzuela, L. (2007). *A survey on control schemes for distributed solar collector fields. Part II: Advanced control approaches.* Solar Energy, 81-10, 1252-1272.

[6] Camacho, E. F., Berenguel, M., Rubio, F. R. and Martínez, D. (2012). *Control of solar energy systems.* Springer-Verlag, London.

[7] Camacho, E. F. and Gallego, A. (2013). *Optimal operation in solar trough plants: A case study.* Solar Energy, 95, 106-117.

[8] Carmona, R., (1985). *Análisis, modelado y control de un campo de colectores solares distribuidos con sistema de seguimiento en eje.* Ph.D. Thesis.

[9] Cirre, C., Berenguel, M., Valenzuela, L. and Camacho, E. F. (2007). *Feedback linearization control for a distributed solar collector field.* Control Engineering Practice, 15-12, 1533-1544.

[10] Cirre, C., Berenguel, M., Valenzuela, L. and Klempous, R. (2009). *Reference governor optimization and control of a distributed solar collector field.* European Journal of Operational Research, 193, 709-717.

[11] Colmenar-Santos, A., Munuera-Perez, F., Tawfik, M. and Castro-Gil, M. (2014). *A simple method for studying the effect of scattering of the performance parameters of parabolic trough collectors on the control of a solar field.* Solar Energy, 99, 215-230.

[12] Gallego, A. and Camacho, E. F. (2012). *Estimation of effective solar irradiation using an unscented kalman filter in a parabolic-trough field.* Solar Energy, 86-12, 3512-3518.

[13] Lima, D., Normey-Rico, J. and Santos, T. (2016). *Temperature control in a solar collector field using filtered dynamic matrix control.* ISA Transactions, 62, 39-49.

[14] Lippke, F. (1995). *Simulation of the part-load behavior of a 30 MWe SEGS plant.* Report No. SAND95-1293, SNL, Albuquerque, NM, USA.

[15] Montes, M., Abánades, A., Martínez-Val, J. and Valdés, M. (2009). *Solar multiple optimization for a solar-only thermal power plant, using oil as heat transfer fluid in the parabolic trough collectors.* Solar Energy, 83-12, 2165-2176.

[16] Navas, S. J., Rubio, F. R., Ollero, P. and Ortega, M. G. (2016). *Modeling and simulation of parabolic trough solar fields with partial radiation.* XV European Control Conference, 31-36.

[17] Price, H., Lupfert, E., Kearney, D., Zarza, E., Cohen, G., Gee, R. and Mahoney, R. (2002). *Advances in parabolic trough solar power technology.* Solar Energy, 124-2, 109-125.

[18] Rubio, F. R., Camacho, E. F. and Berenguel, M. (2014). *Control of solar collector fields.* Revista Iberoamericana de Automática e Informática Industrial (RIAI), 3-4, 26-45.

[19] Shinskey, F. (1978). *Energy conservation through control.* Academic Press.

[20] Smith, R. (2005). *Chemical process design and integration.* Wiley.